

REMOVAL OF SO<sub>2</sub> FROM SIMULATED  
STACK GAS BY Na<sub>2</sub>CO<sub>3</sub> DERIVED FROM MACHOLITE

by

Oliver K. R. Chang

1976

1213-12

ProQuest Number: 10782060

All rights reserved

INFORMATION TO ALL USERS

The quality of this reproduction is dependent upon the quality of the copy submitted.

In the unlikely event that the author did not send a complete manuscript and there are missing pages, these will be noted. Also, if material had to be removed, a note will indicate the deletion.



ProQuest 10782060

Published by ProQuest LLC (2018). Copyright of the Dissertation is held by the Author.

All rights reserved.

This work is protected against unauthorized copying under Title 17, United States Code  
Microform Edition © ProQuest LLC.

ProQuest LLC.  
789 East Eisenhower Parkway  
P.O. Box 1346  
Ann Arbor, MI 48106 – 1346

A Thesis submitted to the Faculty and the Board  
of Trustees of the Colorado School of Mines in partial  
fulfillment of the requirements for the degree of Master  
of Science in Chemical and Petroleum-Refining Engineering.

Signed: Oliver K. R. Chang  
Oliver K. R. Chang

Golden, Colorado

Date: Oct 6, 1976

Approved: Victor F. Yesavage  
Dr. V. F. Yesavage  
Thesis Advisor

P. F. Dickson  
Dr. P. F. Dickson  
Head of Department

Golden, Colorado

Date: Oct 6, 1976

ARTHUR LAKES LIBRARY  
COLORADO SCHOOL of MINES  
GOLDEN, COLORADO 80401

DEDICATION

This thesis is dedicated to  
my Father and Wife

ABSTRACT

A previously designed single particle batch reactor was employed to study the effects of individual components in the SO<sub>2</sub>-porous Na<sub>2</sub>CO<sub>3</sub> noncatalytic reaction system. The system represents a potential method of SO<sub>2</sub> removal by solid scrubbing. The experimental data revealed that absence of moisture drastically reduces the overall reaction rate, and CO<sub>2</sub> and excess oxygen have no effect in this reaction system.

TABLE OF CONTENTS

	page
ABSTRACT . . . . .	iv
INTRODUCTION . . . . .	1
EQUIPMENT . . . . .	11
EXPERIMENTAL PROCEDURE . . . . .	15
Simulation of Flue Gas . . . . .	15
Gas Analysis . . . . .	17
Procedure . . . . .	20
RESULTS . . . . .	24
Run Condition and Data Treatment . . . . .	24
Reproducibility . . . . .	28
Moisture Effects . . . . .	29
CO <sub>2</sub> and Excess Oxygen Effects . . . . .	31
Effective Diffusivity and Tortuosity Factor . . . . .	36
CONCLUSIONS . . . . .	48
RECOMMENDATION FOR FUTHER STUDY . . . . .	49
LITERATURE CITED . . . . .	51
APPENDIX A - GENERALIZED REGRESSION COMPUTER PROGRAM IN MATRIX FORM . . . . .	53
APPENDIX B - THE COMPUTER PROGRAM FOR DIFFUSIVITY AND PLOTTING THE CHARTS OF CONVERSION- TIME RELATIONSHIP . . . . .	63
APPENDIX C - RAW DATA AND CALCULATED RESULTS . . . . .	71

LIST OF FIGURES

Figure	Page
1. Variation of Solid Concentration in Pellet with Radius After a Particular Reaction Time .	6
2. Schematic Flow Diagram of Reactor System . .	14
3. Calibration Curves of SO <sub>2</sub> and CO <sub>2</sub> in 1st Set Packing Column . . . . .	22
4. Calibration Curves of SO <sub>2</sub> and CO <sub>2</sub> in 2nd Set Packing Column . . . . .	23
5. Conversion-Time Relationship of SO <sub>2</sub> and CO <sub>2</sub> for R 2 . . . . .	39
6. Conversion-Time Relationship of SO <sub>2</sub> and CO <sub>2</sub> for R 3 . . . . .	40
7. Conversion-Time Relationship of SO <sub>2</sub> and CO <sub>2</sub> for R 4 . . . . .	41
8. Conversion-Time Relationship of SO <sub>2</sub> and CO <sub>2</sub> for R 5 . . . . .	42
9. Conversion-Time Relationship of SO <sub>2</sub> and CO <sub>2</sub> for R 6 . . . . .	43
10. Conversion-Time Relationship of SO <sub>2</sub> and CO <sub>2</sub> for R 7 . . . . .	44
11. Conversion-Time Relationship of SO <sub>2</sub> and CO <sub>2</sub> for R 8 . . . . .	45
12. Conversion-Time Relationship of SO <sub>2</sub> and CO <sub>2</sub> for R 10 . . . . .	46
13. Conversion-Time Relationship of SO <sub>2</sub> and CO <sub>2</sub> for R 11 . . . . .	47

LIST OF TABLE

Table	Page
1. Run Condition and Results . . . . .	25
2. Reproducibility Results . . . . .	29
3. Data for $D_{Am}$ in a Coal-Fired Power Plant . .	33
4. Tortusosity Factors . . . . .	38
5. Raw Data and Calculated Results for R 2 . .	72
6. Raw Data and Calculated Results for R 3 . .	73
7. Raw Data and Calculated Results for R 4 . .	75
8. Raw Data and Calculated Results for R 5 . .	77
9. Raw Data and Calculated Results for R 6 . .	79
10. Raw Data and Calculated Results for R 7 . .	81
11. Raw Data and Calculated Results for R 8 . .	83
12. Raw Data and Calculated Results for R 10 . .	85
13. Raw Data and Calculated Results for R 11 . .	87

ARTHUR LAKES LIBRARY  
 COLORADO SCHOOL of MINES  
 GOLDEN, COLORADO 80402

## NOMENCLATURE

$C_{Ag}$	Bulk concentration of $SO_2$
$C_{Ai}$	Initial bulk concentration of $SO_2$
$D_e$	Intraparticle effective diffusivity of $SO_2$
$D_K$	Knudsen diffusivity of $SO_2$
$D_{K,eff}$	Effective Knudsen diffusivity of $SO_2$
$D_{12,eff}$	Effective bulk diffusivity of $SO_2$
M.W	Molecular weight of $SO_2$
Pr	Peak ratio
R	Radius of a particle
$r_c$	Radius of unreacted-core
$r_e$	Mean pore radius
t	Time
Temp	Temperature of the reactor
Vr	Volume ratio
$Y_B$	Dimensionless group in equation (4)
$\rho$	Density of solid particle
$\rho_B$	Molar density of the sodium carbonate particle
$O_c$	$r_c/R$
$\epsilon$	Solid void fraction
$\tau$	Tortuosity factor

ACKNOWLEDGEMENTS

I would like to express my sincere thanks to Dr. Yesavage, V. F., my thesis advisor, for his counsel and guidance. I would also like to express my appreciation to Prof. Astle, W. R., and Dr. Hines, A. L. for serving on the thesis committee. The financial support from the National Science Foundation, contract number NSF IG - 4056, is also gratefully acknowledged.

## INTRODUCTION

Noncatalytic, gas-solid reactions are of considerable importance in chemical and metallurgical industries. Gasification or combustion of coal and oil shale, oxidation of sulphur and halogenation of metal are some examples of gas-solid reactions where the size of solid reactant changes with reaction time. A few examples where the gaseous reactants are absent are pyrolysis of carbonaceous materials and thermal decomposition of some organic or inorganic solids. Examples in which the solid does not change appreciably in size during the reaction include the reduction of metallic oxides, the roasting of ores, the nitrogenation of calcium carbide, the regeneration of carbon deposited catalysts, and  $\text{SO}_2$  removal by solid scrubbing.

Kwon in 1974 studied experimentally and theoretically the removal of  $\text{SO}_2$  by  $\text{Na}_2\text{CO}_3$  in a binary system of  $\text{SO}_2$  in air and proposed the system as a single reaction. In many of the industrial operations, however, we often encounter situations in which multiple reactions are involved or a single reaction occurs in a multicomponent system. For example, in a potential process for removal of  $\text{SO}_2$  from stack gas by a solid scrubbing agent, the flue gas contains not only air and sulfur dioxide but

also moisture and carbon dioxide which may affect the efficiency of pollutants removal. It was observed that a marked decrease in the rate of  $\text{SO}_2\text{-Na}_2\text{O}\cdot\text{Al}_2\text{O}_3$  reaction occurs upon the absence of small amounts of water vapor (Krishnan, 1973). In the presence of oxygen, two reactions were involved in  $\text{SO}_2\text{-Na}_2\text{CO}_3$  scrubbing system, ie,  $\text{Na}_2\text{CO}_3 + \text{SO}_2 \rightarrow \text{Na}_2\text{SO}_3 + \text{CO}_2$  and  $\text{Na}_2\text{CO}_3 + \text{SO}_2 + \frac{1}{2}\text{O}_2 \rightarrow \text{Na}_2\text{SO}_4 + \text{CO}_2$ , although Kwon in 1974 reported the former is the major reaction instead of the latter.

The primary objective of this research was to study the effects of individual components in an  $\text{SO}_2$ -porous  $\text{Na}_2\text{CO}_3$  dry scrubbing or noncatalytic, multicomponent reaction system. In addition, the sharp interface shrinking-core model was checked experimentally in this study based on a pore diffusion limited reaction, pseudo-steady state and time-dependent concentrations of gaseous reactants.

In the  $\text{SO}_2$  removal problem, many control techniques have been developed recently, such as: dry and wet absorption, and catalytic oxidation etc. The technical feasibility of some wet processes has been demonstrated. Dry processes are still more in the experimental stage. Many investigators have studied dry  $\text{SO}_2$ -scrubbing agents such as nahcolite, dawsonite, dolomite, alkalized alumina and manganese dioxide. A good literature survey in the subject of this field has been done by Kwon (1974).

The recent energy shortage has stimulated the consideration of major development of unconventional sources of fossil fuels, such as oil shale. The major problems of oil shale development will be in handling the large volume of spent oil shale solids and the impact on the environment. Markets for spent oil shale solids can offset economically the cost of developing oil shale without degradation of environment in ecology and reduce drastically the spent volume for disposal. Such an approach was proposed by Superior Oil Co. to explore the oil shale which contains the minerals nahcolite ( $\text{NaHCO}_3$ ) and dawsonite (Al-compound) in one integrated operation (Weichman, 1974). Weichman in 1974 reported that nahcolite can absorb nearly 100 % of  $\text{SO}_2$  from a stack gas under controlled laboratory conditions and suggested that nahcolite can be dehydrated in heating to produce porous  $\text{Na}_2\text{CO}_3$  for stack gas cleaning. Thus, the  $\text{Na}_2\text{CO}_3$  scrubbing system is potentially applicable to air pollution control. The major advantages of using  $\text{Na}_2\text{CO}_3$  from  $\text{NaHCO}_3$  are added porosity during release of moisture and  $\text{CO}_2$  upon heating and the fact that  $\text{Na}_2\text{CO}_3$  will not absorb  $\text{CO}_2$  which exists in flue gas.

A previously designed single particle batch reactor was employed to run the experiments at conditions:  $120^\circ\text{C}$  constant temperature at ambient pressure, sulfur dioxide

concentrations between 900 ppm and 1.2 % in weight, particle densities from 1.06 gms/cc to 1.34 gms/cc, and particle radius range of 0.32 cm - 0.54 cm. The single particle batch reactor can be a valuable tool in studying gas-solid heterogenous reactions (Kwon and Yesavage, 1976). Advantages of a batch reactor over a continuous flow in this study are the ease of obtaining a large amount of experimental data, the ease of analysis of the experimental data and inherent nature of unsteady state operation since the boundary is moving in gas-solid reactions. A few major limitations of the study are the maximum operating temperature and the allowable sample size.

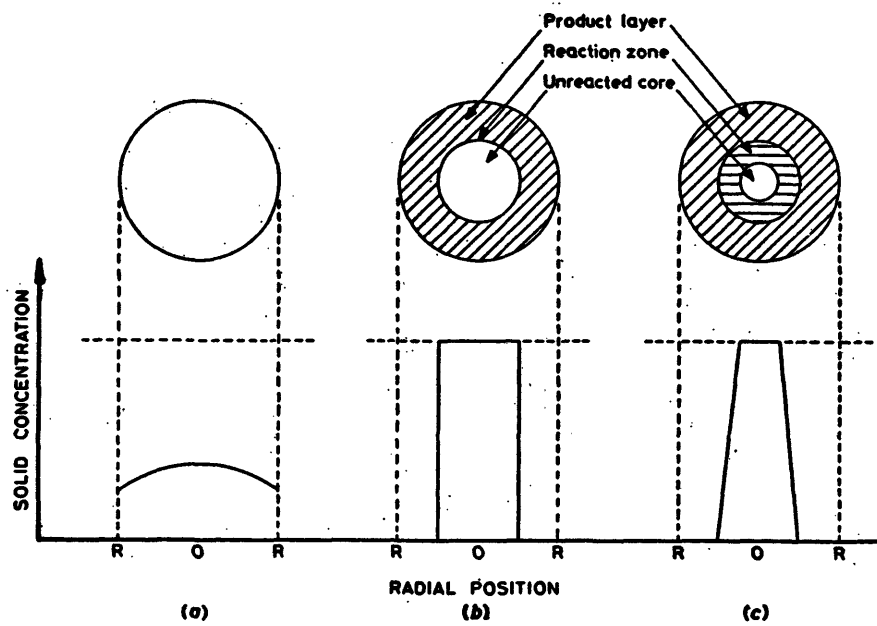
In an example of a coal-fired power plant, stack gas is composed of 76.2 %  $N_2$ , 14.2 %  $CO_2$ , 3.4 % excess oxygen, 6.0 % moisture and trace amount of  $SO_2$  in volume percent (Stern, 1968). Simulation of flue gas is accomplished to determine the effect of individual components on reaction rate of the  $SO_2$ - $Na_2CO_3$  scrubbing system by means of a bomb, a laboratory drying unit, a vacuum pump and a SEKO scale.

Rate expressions for reactions in various systems are normally depicted by mathematical models. The criterion of a model's usefulness in both design and operation of the reacting system is its accuracy without being too complicated mathematically. Sampath et al. in

1973 reviewed with 32 references the applicability of the homogenous model, and the sharp interface and finite thickness reaction zone unreacted shrinking-core models in depicting the kinetics of industrial non-catalytic reactions. These three models are briefly introduced here for the convenience of discussion later.

**HOMOGENEOUS MODEL** (chemical reaction rate controlling) Suppose the solid is so porous that the gas reactant can reach all parts of the solid without diffusion resistance; this is depicted in Fig.1 (a). The reaction may be visualized as occurring throughout the solid phase, although the actual reaction rates at different positions will vary. The key factor here is that the concentration of reactant in the gas phase is the same at any location within the particle.

**SHARP INTERFACE SHRINKING-CORE MODEL** (pore diffusion limited) This model is acceptable when the reactions always occur at the sharp interface (boundary) between the porous ash layer and the unreacted solid core as shown in Fig. 1 (b). There are two types of reaction systems valid for this model. When the unreacted solid is non-porous or the porosity is so small that the solid is practically impervious to the gaseous reactant, the reaction will occur at the interface between the unreacted solid and the porous product layer.



- 1 (a). Homogeneous model
- 1 (b). Sharp interface unreacted shrinking core model
- 1 (c). Finite thickness unreacted shrinking core model

Fig. 1. Variation of solid concentration in pellet with radius after a particular reaction time (Levenspiel, 1962).

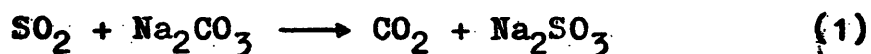
This model is also applicable when the chemical reaction rate is very rapid and the diffusion is sufficiently slow. The concentration of gas reactions at the boundary is practically zero. The zone of reaction in such cases will be confined to the interface between the unreacted solid and the product. However, this model is not applicable when the reacting particles undergo swelling, ablating, cracking, splitting, and sintering (Wen and Wei, 1970).

REACTION ZONE SHRINKING-CORE MODEL (intermediate control) As has been mentioned earlier, total control of reaction rate by either chemical reaction or diffusion characteristics of the system are only extreme cases. The more general situation is where both these steps play a significant role in the overall rate control (Ishida and Wen, 1968. Ausman and Watson, 1962). It is more realistic to assume a narrow but finite thickness reaction zone between the product layer and unreacted core instead of one with a sharp interface as shown in Fig. 1 (c). This in effect means that the diffusing gas does not get consumed immediately on contact with the reaction zone but only after penetration of a small but finite length into the unreacted core. Reaction occurs all over this length. Under extreme conditions of total chemical reaction or diffusion control, this

reaction zone either extends all over the particle or contracts to give a sharp interface.

In this study, the gaseous  $\text{SO}_2$ -porous  $\text{Na}_2\text{CO}_3$  reaction system, the sharp interface shrinking-core model developed by Kwon in 1974 was used. He assumed that the pore diffusion is limiting and the chemical reaction is very fast under isothermal conditions with time-dependent concentration of gas reactants surrounding the spherical particle because of the unsteady operating nature of the batch reactor. Before 1973, all investigators made the assumption that the bulk concentration of gas reactants is constant under a continuous flow study for gas-solid reactions (Sampath et al., 1973).

The reaction in removal of  $\text{SO}_2$  by  $\text{Na}_2\text{CO}_3$  scrubbing agent can be written as follows:



The bulk concentration of  $\text{SO}_2$  can be obtained from a overall material balance in terms of the radius of the unreacted core.

$$C_{Ag} = C_{Ai} - \frac{4\pi R^3}{3V} (1 - \theta_c^3) \quad (2)$$

On the basis of the sharp interface shrinking-core model, the following theoretical equation for the single-particle batch reactor can be derived (Kwon

and Yesavage, 1976).

$$\begin{aligned} \left( \frac{D_e C_{A1}}{R^2 \rho_B} \right) t = & \frac{Y_B^3 + 1}{6Y_B} \ln \left( \frac{(Y_B^3 + 1)(Y_B + \theta_c)^3}{(Y_B + 1)^3 (Y_B^3 + \theta_c^3)} \right) \\ & + \frac{Y_B^3 + 1}{\sqrt{3}Y_B} \left( \tan^{-1} \left( \frac{2 - Y_B}{\sqrt{3}Y_B} \right) - \tan^{-1} \left( \frac{2\theta_c - Y_B}{\sqrt{3}Y_B} \right) \right) \\ & - \frac{(Y_B^3 + 1)}{3} \ln \left( \frac{Y_B^3 + 1}{Y_B^3 + \theta_c^3} \right) \end{aligned} \quad (3)$$

$$\text{where } Y_B^3 = \frac{3VC_{A1}}{4\pi\rho_B R^3} - 1 \quad (4)$$

$$\theta_c = \frac{r_c}{R}$$

A conversion-time relationship was obtained after fitting the experimental data of the reactant gas (SO<sub>2</sub> in the present case) into a modification of equation (3) to get effective diffusivity. This expression can be

applied to determine the intraparticle diffusivity in the ash layer in gas-solid reactions (Gokarn et al., 1972). In addition, the gaseous product,  $\text{CO}_2$ , was measured as a function of elapsed reaction time to compare with the theoretical model fitted by experimental data of  $\text{SO}_2$  since in 1974 Kwon did not analyse the gas product.

### EQUIPMENT

The apparatus used in this study consisted of a batch reactor system plus SO<sub>2</sub> feed unit, a laboratory gas drying unit and a flue gas simulation system. A flow diagram of the equipment is presented in Figure 2. Most of the equipment is made of stainless steel because of the natural corrosive property of sulfur dioxide.

The design and construction of the batch reactor system for this investigation was done by Kwon, 1974. The basic components of the reactor system are a 7,010 ml batch reactor (16) to contain multicomponent reaction mixtures and a single solid particle, an isothermal oil bath (17) to keep the reaction temperature constant at 120°C, a magnetic stirrer (19) to eliminate temperature and mass transfer gradients in the reactor and an SO<sub>2</sub> feed unit (20).

A liquified SO<sub>2</sub> cylinder is connected with a  $\frac{1}{2}$ " coil column of stainless steel which worked as a collection tube for pure SO<sub>2</sub> gas feed. At the other end of the  $\frac{1}{2}$ " coil column is an on-off valve with a silicon rubber stopper for taking pure SO<sub>2</sub> as feed by means of a 30 ml glass syringe.

The W.A. Hammond, 2  $\frac{5}{8}$ " x 11  $\frac{3}{8}$ ", laboratory gas and air drying unit will dry air at pressures up to

90 psig. Indicating drierite in this acrylic unit dries air to a dew point of  $-100^{\circ}\text{F}$  and provides an indication of the dessicant condition. Flow rate may be as great as 200 liters per hour or 0.1 scfm.

The stack gas simulation system consisted of a bomb, a nitrogen cylinder, a carbon dioxide cylinder, a SEKO scale, and a vacuum pump. The SEKO scale is manufactured by Seeder-Koh Busch Inc., New Jersey and weighs up to 10 Kg with an accuracy of 1 mg. Flue gas was simulated in a 1,000 ml stainless steel Hoke bomb with a pressure rating of 3,000 psi. Before simulating flue gas in the bomb, a W. M. Welch vacuum pump was employed to evacuate the bomb to 42.5 cm Hg vacuum.

**Legend to Figure 2.**

<b>Item No.</b>	<b>Description</b>
1	Bomb
2	Labortary gas drying unit
3	Inlet valve
4	Exit valve
5	Temperature controller stirrer
6	Auxiliary stirrer
7	Thermometer
8,11	Vertical rod
9	Sample port, plugged with silicone rubber
10	Horizontal rod
12	Stainless steel plug
13	Hook
14	Platinum net
15	Solid particle
16	Batch reactor
17	Isothermal oil bath
18	Magnetic bar
19	Magnetic stirrer
20	SO <sub>2</sub> feed unit

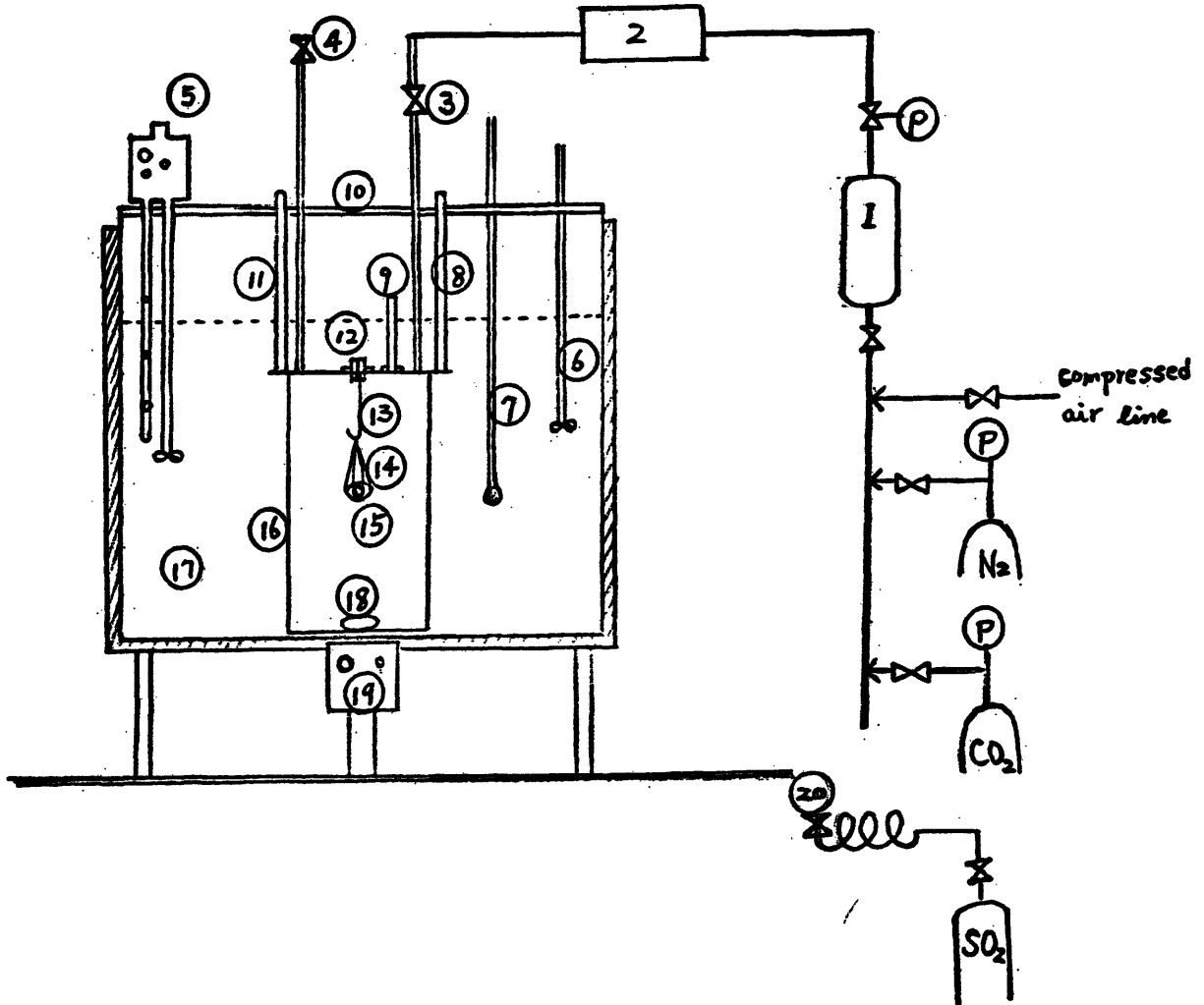


Fig. 2. Schematic flow diagram of reactor system.

### EXPERIMENTAL PROCEDURE

Various combinations of  $N_2$ ,  $CO_2$ ,  $O_2$ , moisture and  $SO_2$  were prepared in the reactor as a simulation of flue gas to study the effects of individual components in the  $SO_2$ -porous  $Na_2CO_3$  reaction system. All experimental runs were done in a random order. Reaction rates were determined in the constant temperature  $120^\circ C$  at ambient pressure, sulfur dioxide concentrations between of 900 ppm and 1.20 % in weight, particle density between of 1.06 and 1.34 gms/cc, and particle radius range of 0.32 cm to 0.54 cm.

The procedures in which they were performed are listed in the following:

- 1) preparation of solid spherical particle
- 2) simulation of flue gas
- 3) gas analysis
- 4) procedure

Among these procedures, preparation of solid particle was given in Kwon, 1974.

#### Simulation of Flue Gas

A typical stack gas stream in a coal-fired power plant is composed of 76.2 %  $N_2$ , 14.2 %  $CO_2$ , 3.4 % excess oxygen, 6.0 % moisture and trace amount of  $SO_2$  in volume percentage. In the flue gas simulation, a mixture of

the components in flue gas: nitrogen and carbon dioxide, was added to the bomb and dried by passage through the drying unit. Given amounts of pure  $\text{SO}_2$  and moisture were directly injected into the reactor by a syringe after the temperature in the oil bath reached a steady  $120^\circ\text{C}$  and the reactor was purged by the mixture of  $\text{N}_2$  and  $\text{CO}_2$  prepared in the bomb. As for the excess oxygen, a compressed air line was connected to the reactor as another experimental run to reproduce data from Kwon's. (1974).

First of all, the bomb was evacuated down to 23.5 cm Hg, indicated by a vacuum gage. The evacuated bomb was weighed on the SEKO scale. Based on the maximum pressure allowable in the bomb, the bomb was first filled with carbon dioxide through a pressure regulator set at the desired pressure to give the desired concentration. The bomb filled with  $\text{CO}_2$  was weighed again to record the weight gain from carbon dioxide. This was repeated with nitrogen to obtain the desired mixture.

When the oil bath reaches  $120^\circ\text{C}$  constant temperature, the mixture of  $\text{CO}_2$  and  $\text{N}_2$  in the bomb was passed through the drying unit and purged the batch reactor. Several samples were taken from the sample port on top of the reactor during purging and injected into the gas chromatograph to check purging. If the purging was accomplished, both the inlet and exit valves of the reactor were closed.

A given amount of  $\text{SO}_2$  from the sulfur dioxide feed unit and water were injected into the reactor.

### Gas Analysis

The analysis of gases was accomplished by an F & M model 720 gas chromatograph with a heated thermal conductivity detector. A 8' x  $\frac{1}{4}$ " Porapak Q column at a temperature of  $125^\circ\text{C}$  separated air first, then carbon dioxide, moisture and sulfur dioxide in order of retention time. Helium as a carrier gas was supplied to the gas chromatograph at a pressure of 10 psig.

During the run, 2.2 ml gas samples were taken from the sample port at different time intervals to measure the concentrations of  $\text{SO}_2$  and  $\text{CO}_2$  as a function of reaction time. When a large amount of carbon dioxide is initially added in the simulated stack gas, the formation of  $\text{CO}_2$  in the reaction is so small compared with the initial presence of  $\text{CO}_2$  that it can not be detected by the gas chromatograph.

To account for variations in detector sensitivity, it is necessary to calibrate the gas chromatograph in terms of peak ratios instead of absolute peak heights. The calibration curve of volume ratio versus peak ratio was made for carbon dioxide and sulfur dioxide, but not for moisture since moisture concentration did not vary

with time during reaction. The calibration was fulfilled by determining an average response peak ratio relative to air and average retention time for each component. Various concentrations of standard samples were prepared in the reactor by injecting successive 10 ml samples of pure gaseous sulfur dioxide and carbon dioxide into the reactor with a 30 cc glass syringe.

Since peak width increases and peak height decreases with increasing retention volume, height measurements offer greater sensitivity for early peaks. Peak ratios of carbon dioxide versus air were calculated on the peak height basis. But peak ratios for sulfur dioxide with respect to air were based on peak area rather than peak height because the fact that peak area remains constant with increasing retention volume ( at constant detector sensitivity ) and consequently offers greater sensitivity for late peaks.

$$\text{peak area of SO}_2 = \text{peak height} \times \text{width at half peak height}$$

The volume ratios of sulfur dioxide and carbon dioxide relative to air can be obtained from the amounts of pure component injected into the reactor, the temperature and pressure of the reactor, and the ambient pressure when the reactor is closed. The method to obtain volume

ratio is simple if the ideal gas law is obeyed.

A generalized multiple regression computer program in matrix form was run to obtain calibration curves for  $\text{SO}_2$  and  $\text{CO}_2$  as shown in Appendix A. The results are:

For the first Porapak Q column:

$$\text{SO}_2: \text{Vr} = 2.81 \times 10^{-3} + 0.77 \text{ Pr} \quad (5)$$

$$\text{CO}_2: \text{Vr} = 2.09 \times 10^{-4} + 1.24 \text{ Pr} \quad (6)$$

and the column for the second packing of Porapak Q:

$$\text{SO}_2: \text{Vr} = 4.59 \times 10^{-4} + 0.95 \text{ Pr} \quad (7)$$

$$\text{CO}_2: \text{Vr} = -7.75 \times 10^{-4} + 1.18 \text{ Pr} \quad (8)$$

where  $\text{Pr}$  = peak ratio of component relative to air

$\text{Vr}$  = volume ratio respect with to air

The second column was required because the first column lost its property for separation of  $\text{CO}_2$  and  $\text{SO}_2$  from air after three months operation. It is physically impossible for concentration below zero to exist as indicated in equation (8). The initial presence of carbon dioxide in the atmosphere caused the negative intercept in equation (8). Figures 3 and 4 presented the calibration curves of carbon dioxide and sulfur dioxide. The minimum

concentration of  $\text{CO}_2$  and  $\text{SO}_2$  which can be detected by gas chromatograph are 300 ppm and 900 ppm, respectively, from the calibration curves in Figures 3 and 4.

### Procedure

The procedure for each run is given below.

- 1) Heat up reactor system to  $120^\circ\text{C}$ . Purge the reactor with dry  $\text{N}_2$ .
- 2) Preheat the single particle in oven at  $120^\circ\text{C}$  for at least one hour and weigh it in digital balance.
- 3) Mount the solid particle on the platinum net and hang the set inside the reactor.
- 4) Add simulated flue gas minus the  $\text{SO}_2$  to the reactor at  $120^\circ\text{C}$  and ambient pressure otherwise  $\text{SO}_2$  will react immediately with particle.
- 5) Submerge the reactor in oil bath and turn on magnetic stirrer in order to eliminate temperature and concentration gradients around the particle.
- 6) 30 ml of pure  $\text{SO}_2$  is injected into reactor with a 30 ml glass syringe. Immediately take a 2.2 ml gas sample from sample port using 3 ml plastic syringe and inject into gas chromatograph measured as initial concentration of  $\text{SO}_2$  of around 1.2 wt %.
- 7) During the reaction, take 2.2 ml gas sample at different time intervals until  $\text{SO}_2$  can not be detected.

8) At the end of experiment, controlling heater and magnetic stirrer are turned off and the partially reacted particle is taken out. Purge the reactor with  $N_2$  for the next run.

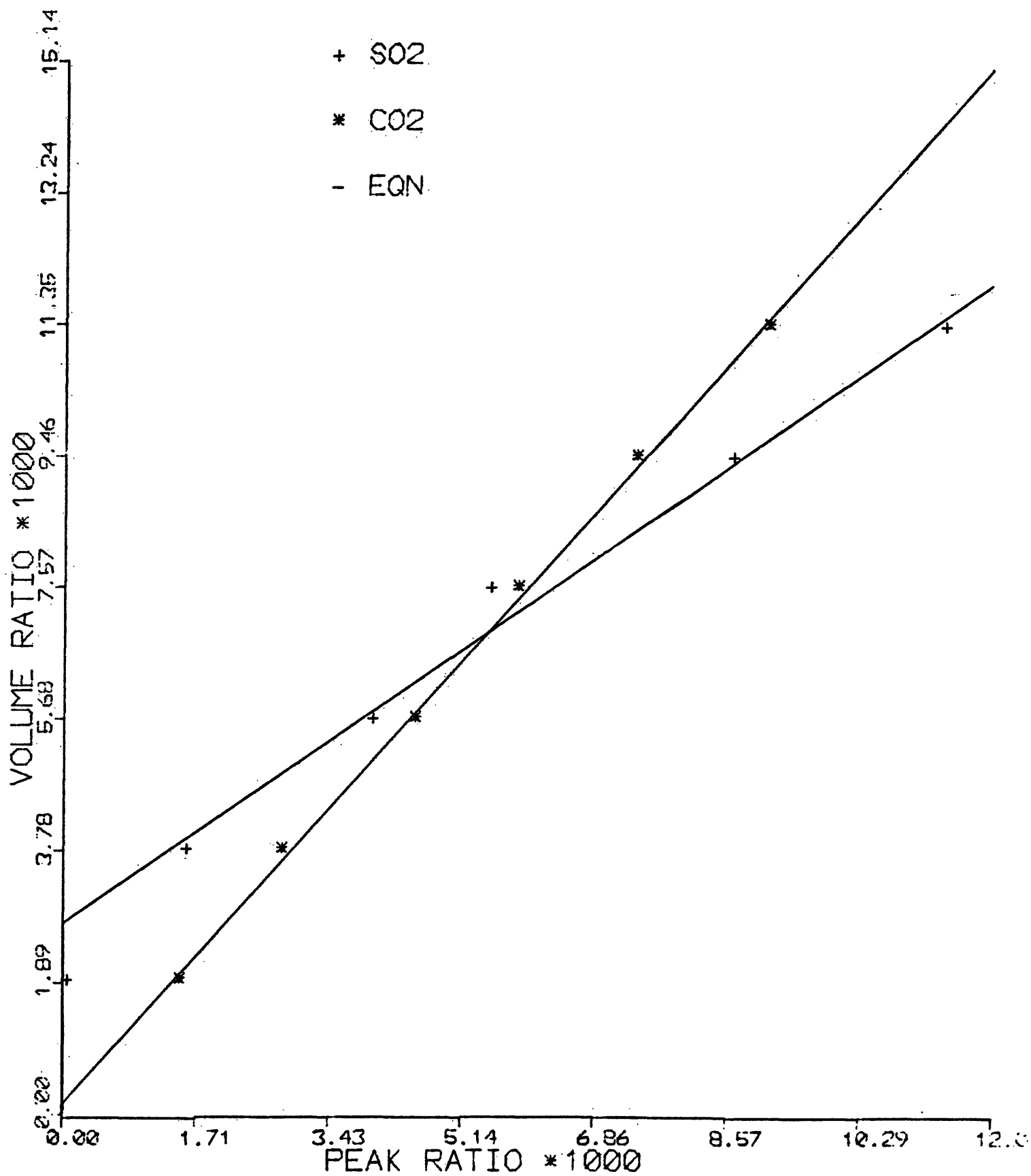


Fig. 3 Calibration curves of CO<sub>2</sub> and SO<sub>2</sub> in 1<sup>st</sup> set packing column.

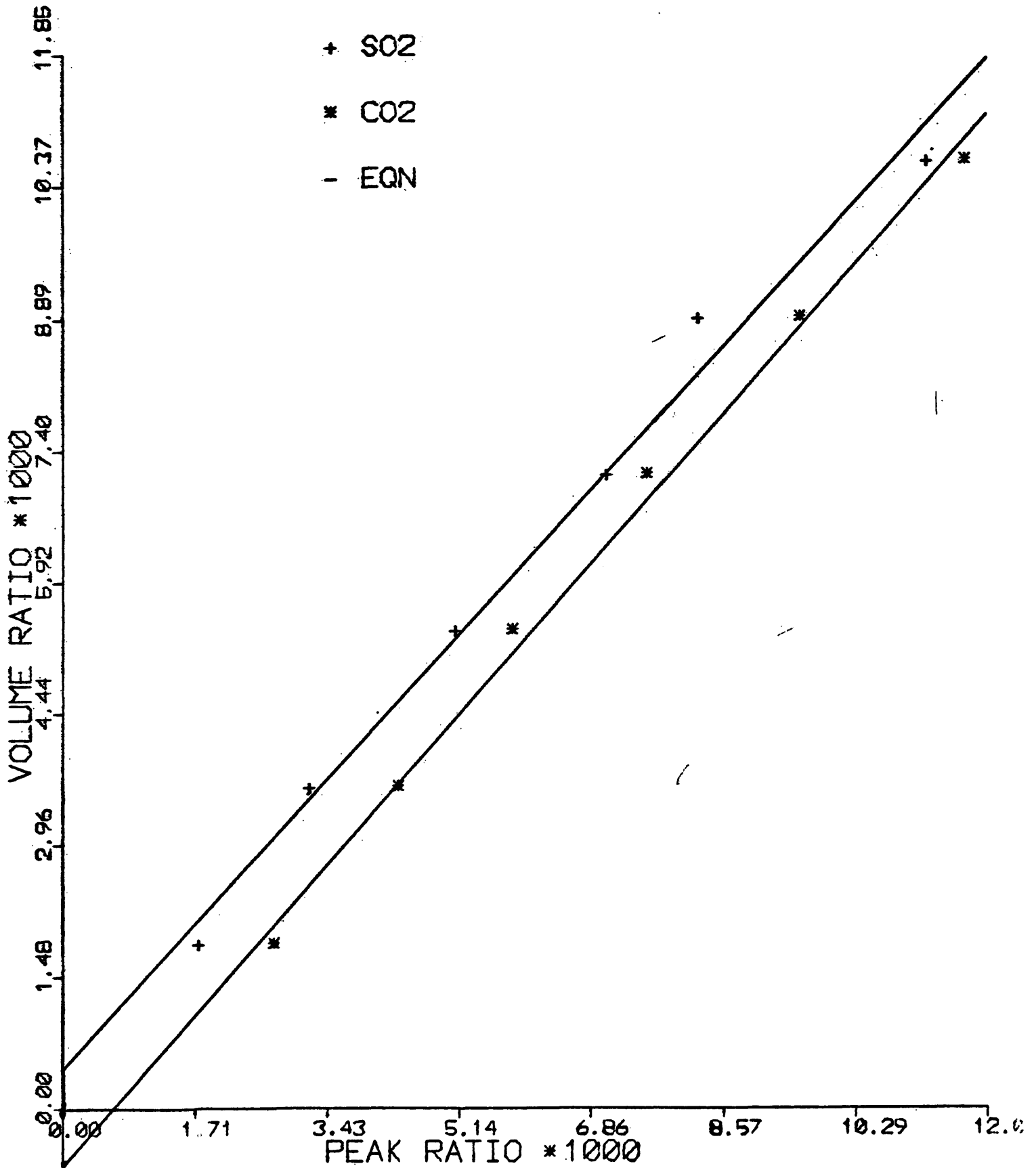


Fig. 4. Calibration curves of CO<sub>2</sub> and SO<sub>2</sub> in 2<sup>nd</sup> set packing column.

## RESULTS

This section presents the experimental results and a discussion of their significance.

### Run Conditions and Data Treatment

Table 1. shows the experimental run numbers and corresponding reaction conditions. All of the runs were carried out at the 120°C constant temperature, ambient pressure, and the initial concentration of SO<sub>2</sub> around 1.2 wt %. Runs 2-7 were all performed in the dry state. The rest were studied in the presence of H<sub>2</sub>O for the moisture effects in the reaction system.

Factors involved in multicomponent reaction systems are very complicated. The effects of individual components in SO<sub>2</sub>-Na<sub>2</sub>CO<sub>3</sub> reaction system were studied by isolation of individual components in the batch reactor. The pair of experiments R 3 and R 8 were designed to study the moisture effects while the runs: R 4, R 6, and R 7 were attempted to investigate the counterdiffusion effects of CO<sub>2</sub>. R 8, R 10, and R 11 were carried out for the effects of excess oxygen. The purpose of R 10 and R 11 was intended to reproduce the data from Kwon's (1974).

Before fitting the experimental data into equation (3), on the basis of a pore diffusion model, a time delay

Table 1. Run Conditions and Results

<u>Number of Experiment</u>	<u>Particle Density (gms/cc)</u>	<u>Particle Radius (cm)</u>	<u>Mixtures in Reaction System</u>	<u>Effective Diffusivity (cm<sup>2</sup>/min)</u>	<u>Confidence Interval of Effective Diffusivity (cm<sup>2</sup>/min)</u>	<u>Time Delay (min)</u>
R 2	1.281	0.546	Dry N <sub>2</sub>	0.049	0.069 - 0.027	1.37
R 3	1.343	0.426	Dry N <sub>2</sub>	0.019	0.035 - 0.003	1.63
R 4	1.279	0.440	0.12 wt % CO <sub>2</sub> in dry N <sub>2</sub>	0.071	0.094 - 0.048	1.64
R 5	1.278	0.443	Dry air	0.006	0.009 - 0.003	0.27
R 6	1.204	0.436	8.34 wt % CO <sub>2</sub> in dry N <sub>2</sub>	0.018	0.026 - 0.010	1.76
R 7	1.283	0.533	13.23 wt % CO <sub>2</sub> in dry N <sub>2</sub>	0.039	0.046 - 0.032	1.93
R 8	1.218	0.497	7.25 wt % H <sub>2</sub> O in N <sub>2</sub>	0.458	0.639 - 0.277	2.23
R 10	1.073	0.422	40 % relative humidity of air	0.718	0.932 - 0.504	10.9
R 11	1.065	0.328	40 % relative humidity of air	2.006	2.249 - 1.751	11.2

was introduced to calculate the effective diffusivity of  $\text{SO}_2$  in  $\text{SO}_2$ -porous  $\text{Na}_2\text{CO}_3$  reaction system (Kwon, 1974). Intraparticle diffusion control is assumed at the beginning of the experiment, but the pore diffusion path is negligible for a short time after reaction starts. Thus, the intraparticle diffusion model used for all times predicts too rapid conversions for short times, when chemical reaction or gas film diffusion always controls. The time delay was generally a small positive correction (less than twelve minutes) for runs lasting as long as 10 hours.

The resultant equation (9) was obtained after introducing the time delay contribution term  $D_e t_d$  into equation (3).

$$y/t = D_e - ( D_e t_d )/t \quad (9)$$

where  $y$  is the right hand side of equation (3) multiplied by  $( R^2 P_B )/C_{A1}$ .

By applying least squares to equation (9),  $D_e$  and  $t_d$  were determined for each experimental run as shown in Appendix B. For the confidence intervals of  $D_e$ , student  $t$  distribution with degree of freedom of (sample number - 2) was used on the basis of 95 % significance level since the sample size is less than 30. The cal-

culating results are presented in Table 1.

Putting the value of  $D_e$  determined from the above method back equation (9), a conversion-time relationship of  $SO_2$  was given for each run. Also the conversion-time relationship for  $CO_2$  can be derived from the mass balance of reaction (1). The resultant curves of  $SO_2$  and  $CO_2$  are plotted in Figures 5-13 by the Houston plotter.

(SUBROUTINE PLOTTER as shown in Appendix B)

From the results in Table 1, it is obvious that moisture holds a pronounced effects in the reaction system of this study. In the dry state, the  $SO_2$ -porous  $Na_2CO_3$  noncatalytic reaction is controlled either by the chemical reaction step solely or by both the pore diffusion and the chemical reaction simultaneously (The detail will be discussed later). As shown in Figures 7-9, the experimental data can not fit the pore diffusion model. This suggests that there is a difference between the chemical kinetics model and the pore diffusion model.

A major problem in applied kinetics is sometimes the inability to distinguish between alternative control mechanisms. Often, the difference in fit may be so slight that it is very difficult to determine whether it is simply due to experimental error or truly due to the difference in mechanism. Furthermore, an alternative mechanism may fit data equally well. For example, the experimental

data of  $\text{SO}_2$  and  $\text{CO}_2$  in Figures 5 and 6 showed good agreement with the theoretical model on the basis of pore diffusion controlling, though the model is wrong in the absence of  $\text{H}_2\text{O}$ .

In the presence of  $\text{H}_2\text{O}$ , the chemical reaction is rapid and the pore diffusion is limited. The experimental data of  $\text{SO}_2$  for R 8, R 10, and R 11 has good agreement with the sharp interface shrinking-core model due to pore diffusion controlling step as shown in Fig. 11-13. The slight deviation of  $\text{CO}_2$  data from the pore diffusion model in Figures 12-13 may be contributed from the experimental errors and the mass balance between  $\text{CO}_2$  and  $\text{SO}_2$ .

#### Reproducibility

The purpose of runs 10 and 11 was intended to reproduce the data from Kwon's (1974) and showed the validity of the sharp interface shrinking-core model. All of those runs were studied in normal humidity of air systems. Table 2 presented the reproducibility results. At the fifth column of Table 2, the calculated effective diffusivity was obtained from the linear regression equation around 2.4 wt % initial concentration of  $\text{SO}_2$  (Kwon, 1974).

$$D_e = 5.785 - 4.131 \rho \quad (10)$$

**Table 2.**  
**Reproducibility Results**

<u>Run Number</u>	<u>Particle Density (gms/cc)</u>	<u>Particle Radius (cm)</u>	<u>Effective Diffusivity (cm<sup>2</sup>/min)</u>	<u>Calculated Effective Diffusivity</u>
R 10	1.073	0.422	0.718	1.35
R 11	1.065	0.328	2.006	1.38
*T 3	1.007	0.378	2.205	1.62
*G 17	1.249	0.315	0.675	0.62

\*from Kwon's data in 1974.

The difference between the values in 4<sup>th</sup> and 5<sup>th</sup> column in Table 2 suggests that the extrapolated linear regression equation (10) from 2.4 wt % initial concentration of SO<sub>2</sub> down to 1.2 wt % in this study can not exactly predict the effective diffusivity in SO<sub>2</sub>-Na<sub>2</sub>CO<sub>3</sub> reaction system. Also the difference was partially contributed from the unavoidable intrinsic scatter of the experimental data.

#### Moisture Effects

The moisture effects in SO<sub>2</sub>-Na<sub>2</sub>CO<sub>3</sub> reaction system was investigated at moisture content of 7.25 wt % and 40 % relative humidity at room temperature, respectively, in N<sub>2</sub> and air system. As showing in the fifth column in Table 1, the calculated  $D_{A,eff}$  for SO<sub>2</sub> increase drastically

from the average magnitude of order  $10^{-1.5}$  in the dry state to that of order  $10^{0.15}$  in the moisture mixture. This strongly indicates that moisture plays an important role in this reaction system. It is in agreement with the reports by Krishnan et al. (1973) and Meyer et al. (1971).

In the removal of  $\text{SO}_2$  by a solid scrubbing agent with  $\text{H}_2\text{O}$  vapor, sulfur dioxide adsorption is enhanced by partial hydrolysis of the solid surface. Water, released during sulfur dioxide adsorption, acts as a catalyst for  $\text{SO}_2$  adsorption (Meyer et al., 1971). In the reports from Krishnan et al. (1973) who studied kinetics of removal  $\text{SO}_2$  by alkalized alumina between  $300^\circ\text{C}$  and  $600^\circ\text{C}$ , water vapors acts catalytically. There was no difference in the X-ray diffraction spectra of sodium sulfate formed after reaction in moisture or dry gases. Furthermore, only a small amount of moisture is required. Also in a scanning electron micrographs of specimen fracture surfaces taken after reaction in dry and  $\text{H}_2\text{O}$  vapor the specific surface of the specimen ( $\text{m}^2/\text{g}$ ) almost reduced in half upon the absence of moisture. The reduction in specific surface of the specimens is more pronounced at lower reaction temperatures. These observations suggest that in the absence of water vapor, the solid reaction product blocks pores, thereby reducing the

available surface area for continued reaction.

Chemically, the molecules of  $\text{SO}_2$  and  $\text{H}_2\text{O}$  are combined together to form a variety of intermediates because of the strong polarity of both  $\text{SO}_2$  and  $\text{H}_2\text{O}$  molecules and the phase equilibrium data of S-compound specimens in  $\text{H}_2\text{O}$ . The intermediates are adsorbed more easily on the surface of solid than  $\text{SO}_2$  does alone. Water is released as catalyst for the next cycle after the intermediates react with the solid reactants.

In other words, the sharp interface shrinking-core model due to pore diffusion limitation can't be applied in the dry state for this reaction system since the chemical reaction is not rapid and the pore diffusion limitation does no longer hold. In the absence of water, the pore diffusion control switches to chemical reaction rate controlling.

#### $\text{CO}_2$ and Excess Oxygen Effects

Initial attempts to isolate the moisture factors from the reaction system to study  $\text{CO}_2$  influence in a dry reaction system proved unsuccessful. The model on the basis of the pore diffusion limited is not valid for reaction in the absence of water vapor. That is the reasons why the fit of experimental data in Figures 7-9 looks no good. As shown in Figure 9 and 10, it is

hard to measure the formation of  $\text{CO}_2$  in the reaction when a large amount of  $\text{CO}_2$  is initially added in the reaction system. Physically, the variation of effective diffusivity of  $\text{SO}_2$  in multicomponent system contributed from the oxygen and  $\text{CO}_2$  present is explained in the following discussion and calculation in terms of Knudsen diffusivity and bulk diffusivity from equation (12).

In a multicomponent mixture, bulk diffusivity depends not only on the nature and concentration but on the fluxes of the species present. As for Knudsen diffusivity, it does not depend on the nature of the species present since only collision with walls are involved, and not those with other molecules. ie,  $D_{k,eff}$  is the same in either binary or multicomponent system.

Table 3 lists the component composition of stack gas in volume and mole percentages in a typical coal-fired power plant, the corresponding symbol for the convenience of discussion,  $D_{A,j}$  of  $\text{SO}_2$  in j binary system, and the fluxes.

$D_{Am}$  represents the bulk diffusivity of  $\text{SO}_2$  in a multicomponent reaction system. Comparing with the flux of  $\text{SO}_2$ , the fluxes of  $\text{H}_2\text{O}$  and  $\text{O}_2$  are small and approximately zero even if they are involved in the chemical reactions.

Table 3

Data for  $D_{Am}$  in a coal-fired power plant

element	SO <sub>2</sub>	CO <sub>2</sub>	H <sub>2</sub> O	O <sub>2</sub>	N <sub>2</sub>
symbol	A	B	C	D	E
*vol %	0.2	14.2	6.0	3.4	76.2
mol % (Y <sub>j</sub> )	0.2	14.2	6.0	3.4	76.2
@(D <sub>Aj</sub> ) Bulk diffusivity of SO <sub>2</sub> in binary mix.	—	0.146	0.204	0.203	0.210
#Flux (N <sub>j</sub> )	N <sub>A</sub> + N <sub>B</sub> = 0		0	0	0

\* from Stern, 1968.

@ from Bird et al., 1970.

# from equalmolar counterdiffusion  
of gases

The bulk diffusivity of A in a multicomponent mixture,  $D_{Am}$ , can be calculated from the following equation (Sherwood et al., 1975).

$$D_{Am} = \frac{N_A - Y_A \sum_{j=1}^{n=5} N_j}{\sum_{j=1}^{n=5} \frac{N_A Y_j - N_j Y_A}{D_{Aj}}} \quad (11)$$

From the data in Table 3, we have

$$D_{Am} = 11.82 \text{ cm}^2/\text{min} \text{ or } 0.197 \text{ cm}^2/\text{sec}$$

Comparing  $D_{A,air}$  (15.548  $\text{cm}^2/\text{min}$ ) with  $D_{Am}$ , the bulk diffusivity of  $\text{SO}_2$  was reduced about 24 % due to the presence of  $\text{O}_2$  and  $\text{CO}_2$ . Since  $\epsilon < 1$  and  $\tau > 1$  from Table 4, the corresponding effective diffusivity should be less than 24 % from equation (12) and (14). Therefore, the effective diffusivity of  $\text{SO}_2$  in the  $\text{SO}_2\text{-Na}_2\text{CO}_3$  multicomponent reaction system can be approximated by that of  $\text{SO}_2$  in air mixture. In other words,  $\text{CO}_2$  diffuses out and retards the diffusion rate of  $\text{SO}_2$  into the particle immediately after  $\text{SO}_2$  reacts with the solid reactant at the interface. This estimation suggests that the counterdiffusion effect of  $\text{CO}_2$  is negligible.

The only effect of  $\text{CO}_2$  that concerns us significantly is the build-up of the concentration of  $\text{CO}_2$  around the surface of the particle to a high enough value to cause the reaction (1) to become reversible. But from the viewpoint of thermodynamics, the equilibrium constant is very small calculated from the free energy of formation. Therefore, the reversible reaction is almost impossible to occur.

If oxygen takes part in the  $\text{SO}_2\text{-Na}_2\text{CO}_3$  reaction system, two additional simultaneous reactions may be involved at  $120^\circ\text{C}$  and 1 atm.

1).  $\text{Na}_2\text{SO}_3 + \frac{1}{2} \text{O}_2 \longrightarrow \text{Na}_2\text{SO}_4$ . In the investigation of reaction kinetics of sodium sulfite oxidation by Barron et al. (1966), it came out that the apparent activation energy was calculated to be 18.3 kcal/g-mole and the value of reaction constant is  $0.065 \text{ (lit)}^{\frac{1}{2}} / (\text{g-mole})^{\frac{1}{2}} (\text{sec})$  in the reaction as zero order in oxygen and three-halves order in sulfite. Also Kwon in 1974 reported that this reaction is very slow. In his analysis of the reacted particle, the average conversion ratio is 6.17 % sulfate to total sulfite plus sulfate in  $\text{SO}_2\text{-Na}_2\text{CO}_3$  reaction in air mixture in which solid product  $\text{Na}_2\text{SO}_3$  is subsequently oxidized to the sulfate. Since the ratio of the volume and the surface of a spherical particle is constant, sulfate may be created on the surface of the particle. This consecutive reaction, therefore, can not affect the pore size and retard the main reaction (1) at the interface between the solid product layer and the unreacted solid reactant if the densities of the reactant solid and the product solid are almost the same.

2)  $\text{SO}_2 + \frac{1}{2} \text{O}_2 \longrightarrow \text{SO}_3$ . Actually the oxidation of  $\text{SO}_2$  proceeds slowly at low temperature ( Here at  $120^\circ\text{C}$  compared with the flame temperature ) in the absence of catalyst, although the equilibrium constant ended up  $10^5$  calculated by Hougen et al. (1962). The effect of oxygen in the waste gases on the conversion of  $\text{SO}_2$  to

$\text{SO}_3$  stands about 5 % of sulfur content in coals or residual oils but most of the  $\text{SO}_3$  formation results from some catalytic action ( Stern, 1968 ). This suggests that the extent of  $\text{SO}_2$  oxidation due to oxygen in the absence of catalyst with the main reaction (1) is very small in this study.

From the stoichometric relationship in the main reaction (1), the moles of  $\text{SO}_2$  consumed should be equal to the moles of  $\text{CO}_2$  yield. The experimental data of  $\text{CO}_2$  for R 8 in  $\text{N}_2$  show in good agreement with the theoretical conversion-time relationship for the intraparticle diffusion model as shown in Figure 11, while the carbon dioxide data for R 10 and R 11 in the air system has no good agreement with the theoretical model as shown in Figures 12 and 13. The difference in fit are so slight in Figures 12 and 13 that it is very difficult to determine whether it is simply due to the experimental error or truly due to the oxidation of  $\text{SO}_2$  by oxygen into the form of  $\text{SO}_3$ .

#### Effective Diffusivity and Tortuosity Factor

Considering all the variables for this reaction system, Kwon in 1974 assumed that the intraparticle effective diffusivity is a function of particle size, particle density, initial  $\text{SO}_2$  concentration and operating temperature. In his work, he concluded that particle

density exerted the strongest influence on intraparticle effective diffusivity among other variables. From this result tortuosity factors can be determined using the equations (12, 13, 14) as described by Satterfield, 1970. For equimolar counterdiffusion of gases within the particle, we have

$$\frac{1}{D_e} = \frac{1}{D_{k,eff}} + \frac{1}{D_{12,eff}} \quad (12)$$

And

$$D_{k,eff} = \frac{D_k \epsilon}{\tau} \quad (13)$$

$$D_{12,eff} = \frac{D_{12} \epsilon}{\tau} \quad (14)$$

where  $D_{12}$  = The diffusivity of  $SO_2$  in air at  $120^\circ C$   
and 1 atm.

$$= 15.54 \text{ cm}^2/\text{min} \text{ (Bird et al., 1970)}$$

$D_k$  = The Knudsen diffusivity of  $SO_2$  in a  
straight round pore.

$$= 9700 \text{ re } \sqrt{\text{Temp}/M.W} \times 60 \text{ (Satterfield, 1970)}$$

Substituting eqns. (13), (14) into eqn. (12), equation (12) becomes

$$\frac{1}{\tau} = \frac{D_e}{\epsilon} \left( \frac{1}{15.548} + \frac{6.93}{r_e} \times 10^{-8} \right) \quad (15)$$

The void fraction of a solid particle can be obtained from the density of nonporous  $\text{Na}_2\text{CO}_3$ , 2.533 gms/cc, and the density of the particle.

$$\epsilon = (2.533 - \rho) / 2.533 \quad (16)$$

Kwon in 1974 established a linear regression relationship between particle densities and  $D_e$  at 125°C as equation (10).

Therefore, the following equation represents the tortuosity factor as a function of particle density and mean pore radius.

$$\frac{1}{\tau} = \frac{(5.785 - 4.131\rho)}{(2.533 - \rho)} \left( 0.163 + \frac{1.75}{r_e} \times 10^{-7} \right) \quad (17)$$

The results are shown in Table 4.

Table 4  
Tortuosity Factors

$\rho$ (gms/cc) \ / \ $r_e$ (Å)	1	1.3
10	0.48	2.97
50	1.81	5.79
500	4.68	15.01
5000	5.56	17.85

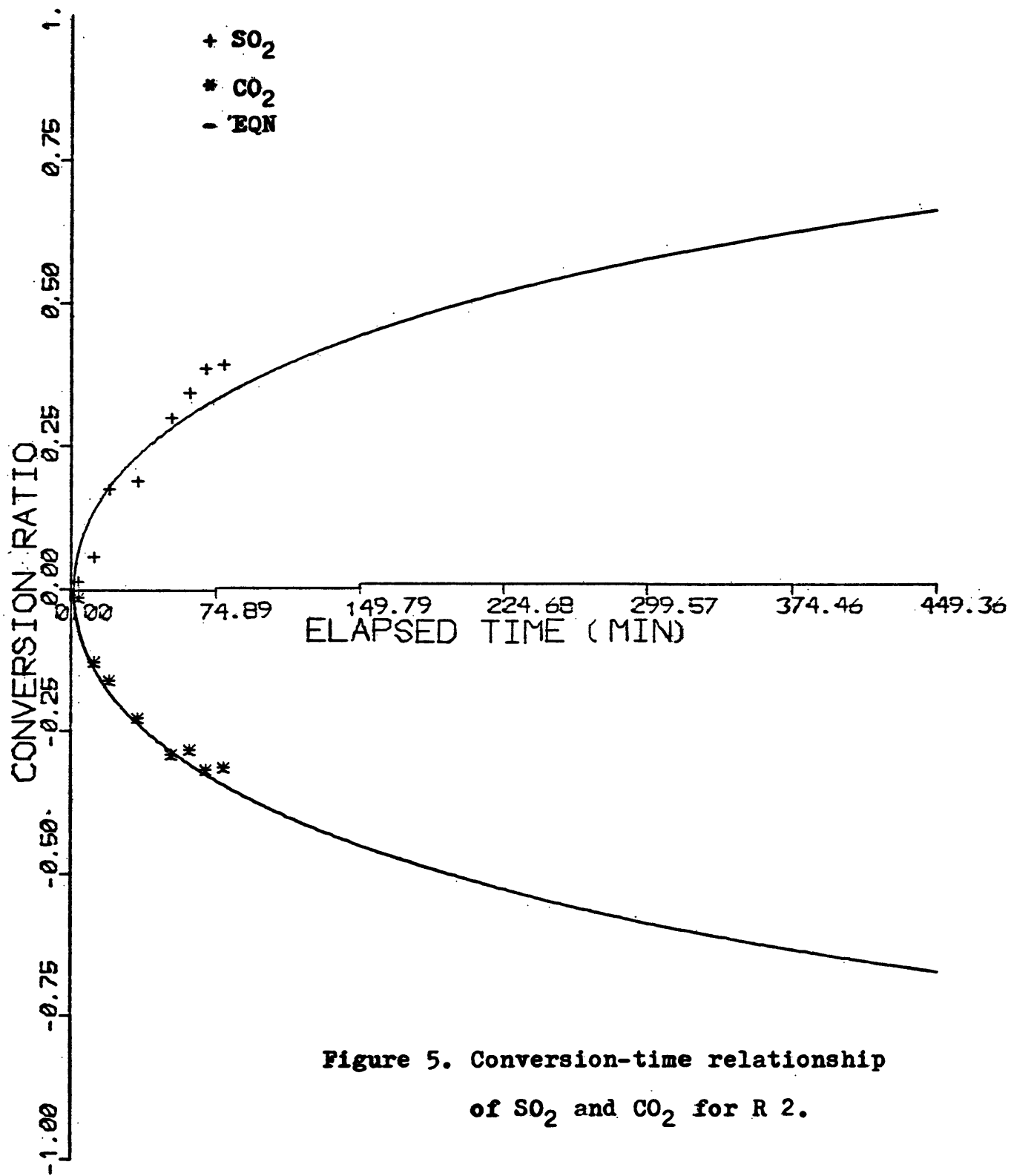


Figure 5. Conversion-time relationship of SO<sub>2</sub> and CO<sub>2</sub> for R 2.

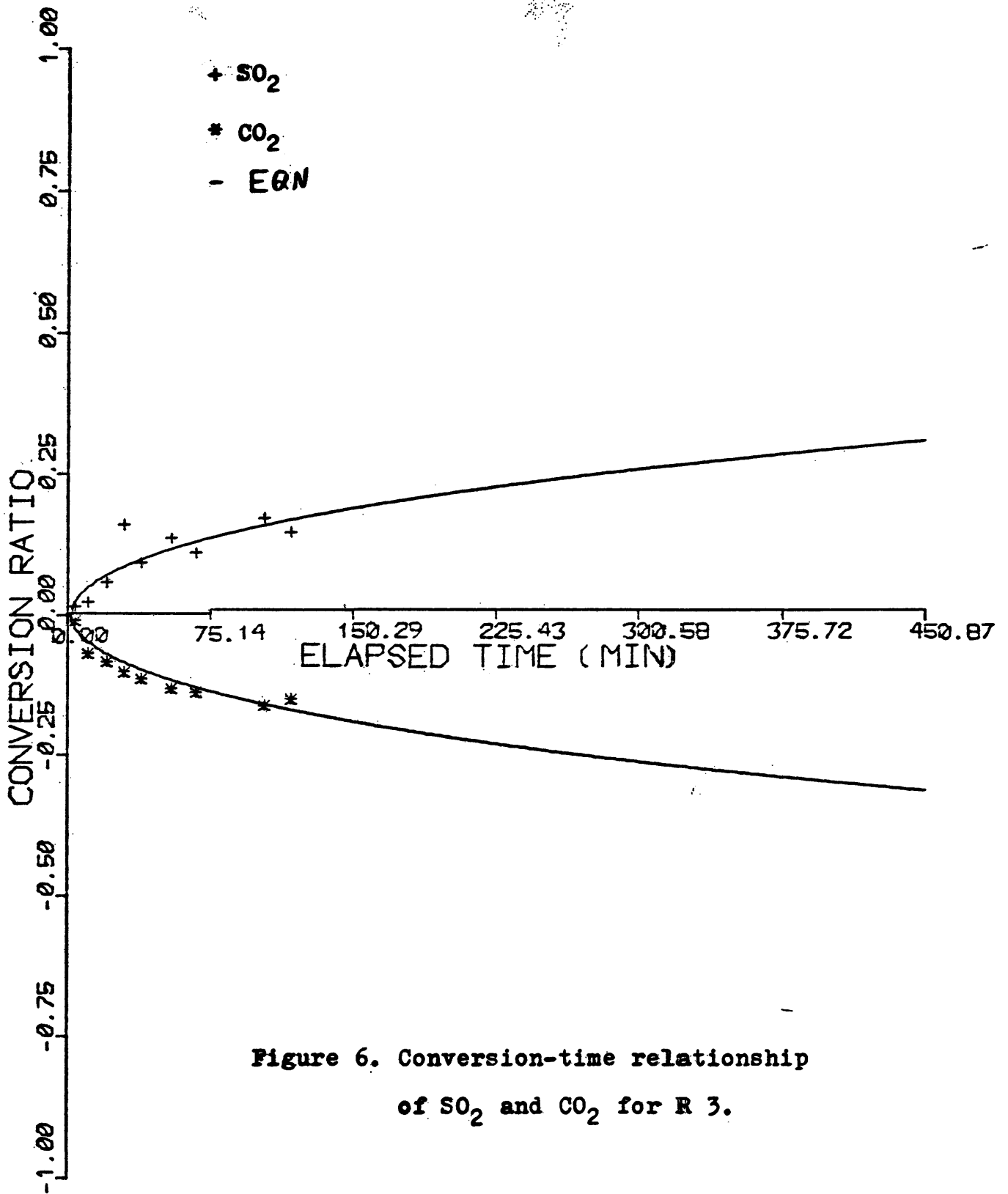


Figure 6. Conversion-time relationship of SO<sub>2</sub> and CO<sub>2</sub> for R 3.

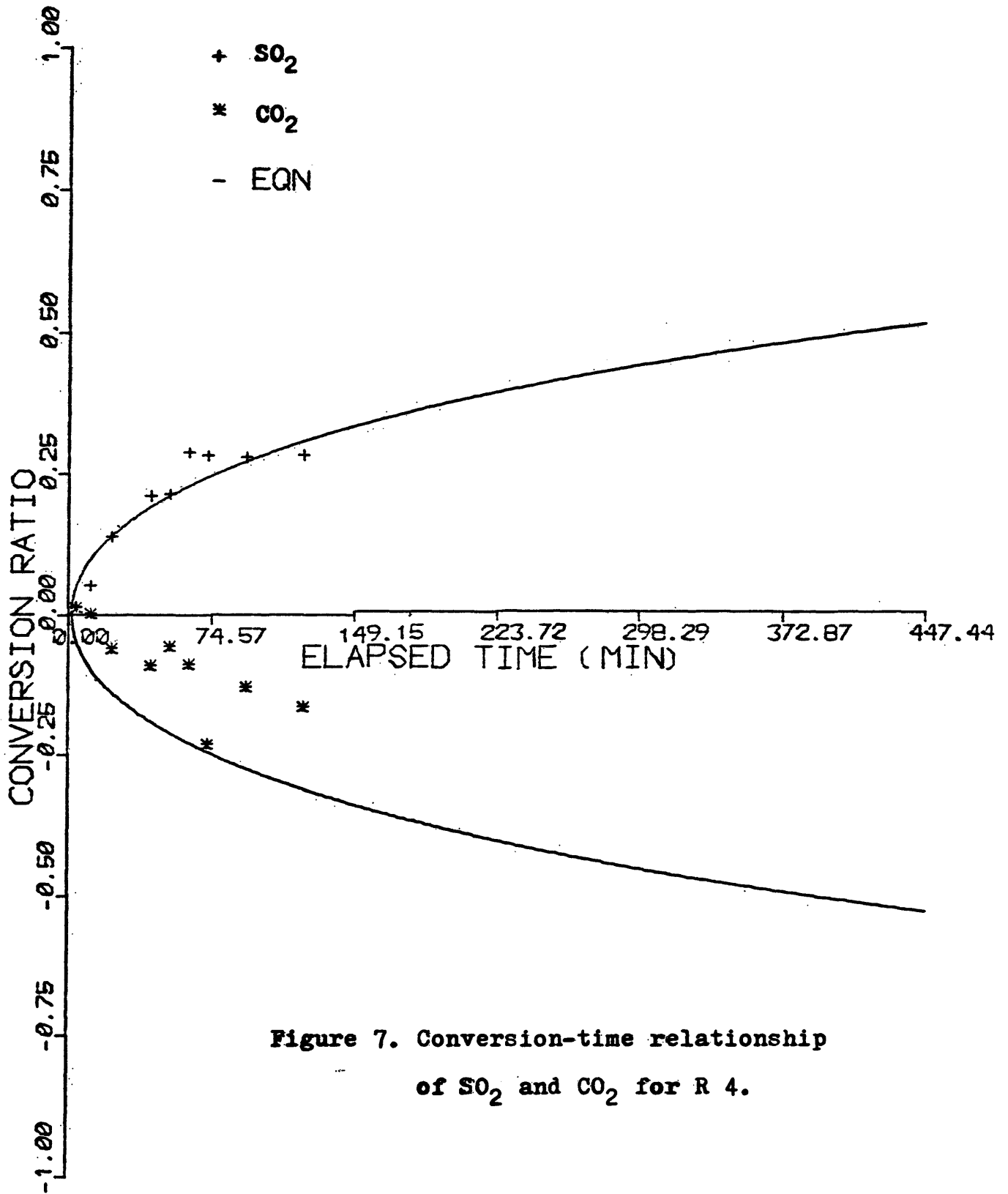


Figure 7. Conversion-time relationship of SO<sub>2</sub> and CO<sub>2</sub> for R 4.

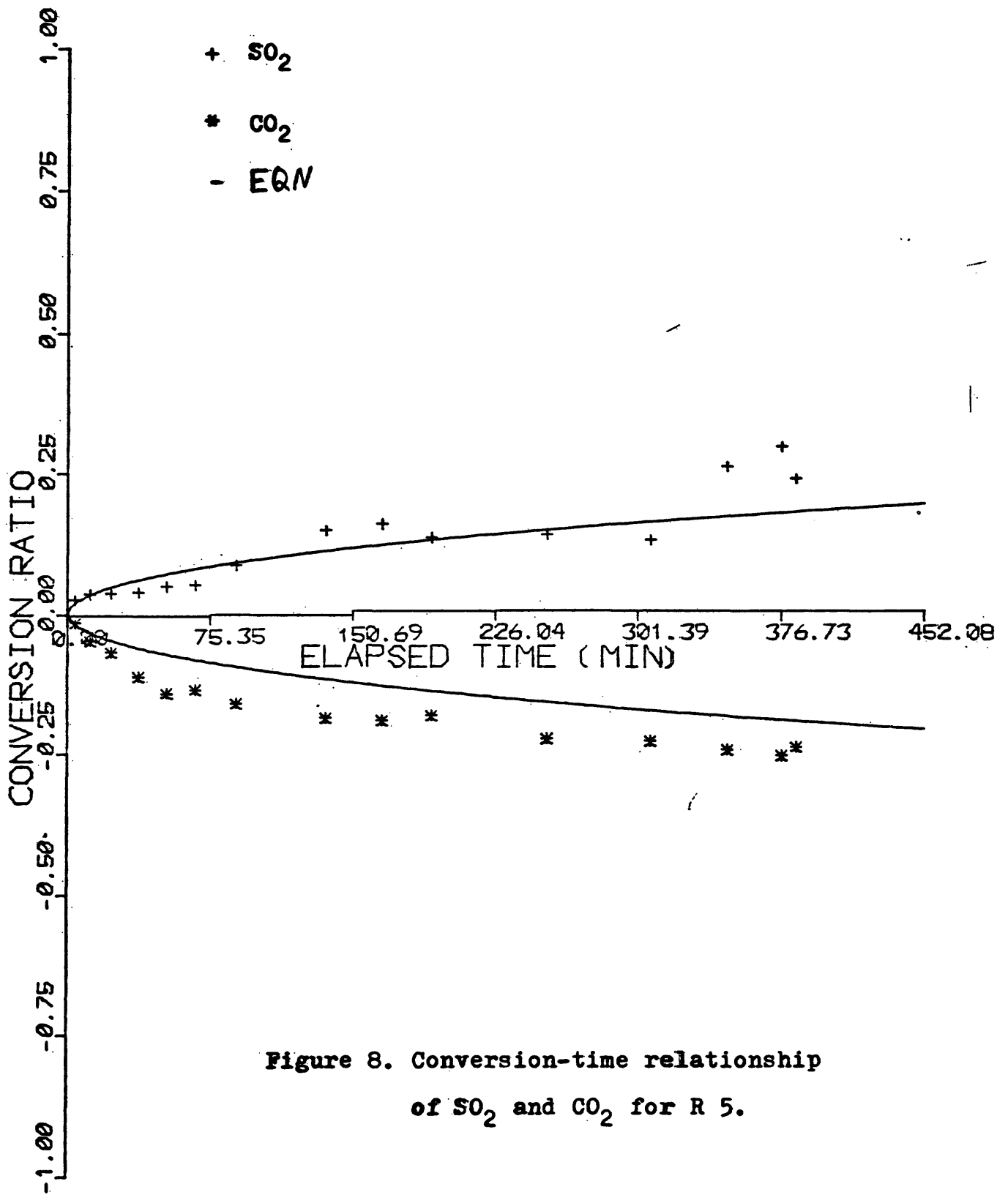


Figure 8. Conversion-time relationship of SO<sub>2</sub> and CO<sub>2</sub> for R 5.

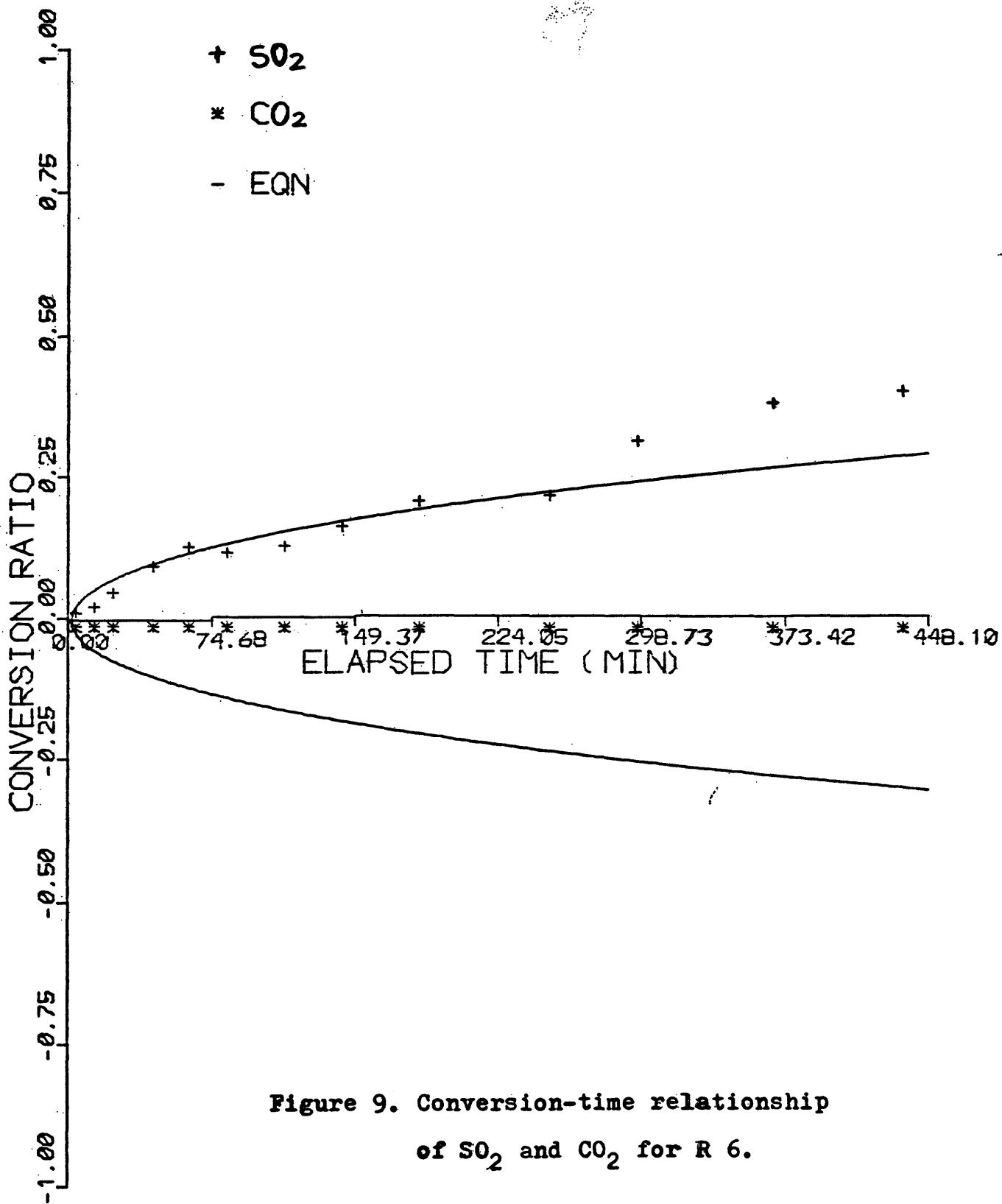


Figure 9. Conversion-time relationship of SO<sub>2</sub> and CO<sub>2</sub> for R 6.

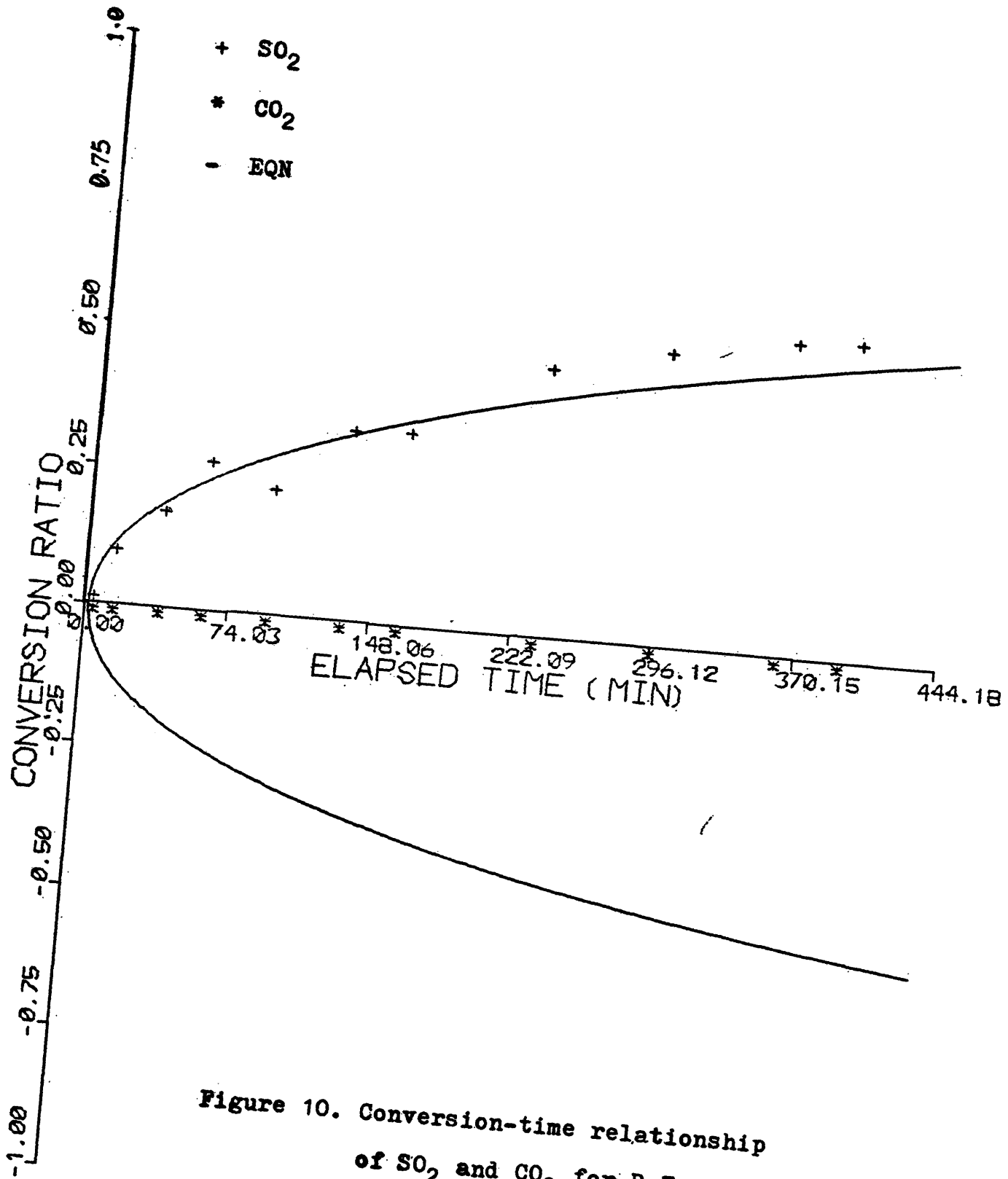


Figure 10. Conversion-time relationship of SO<sub>2</sub> and CO<sub>2</sub> for R 7.

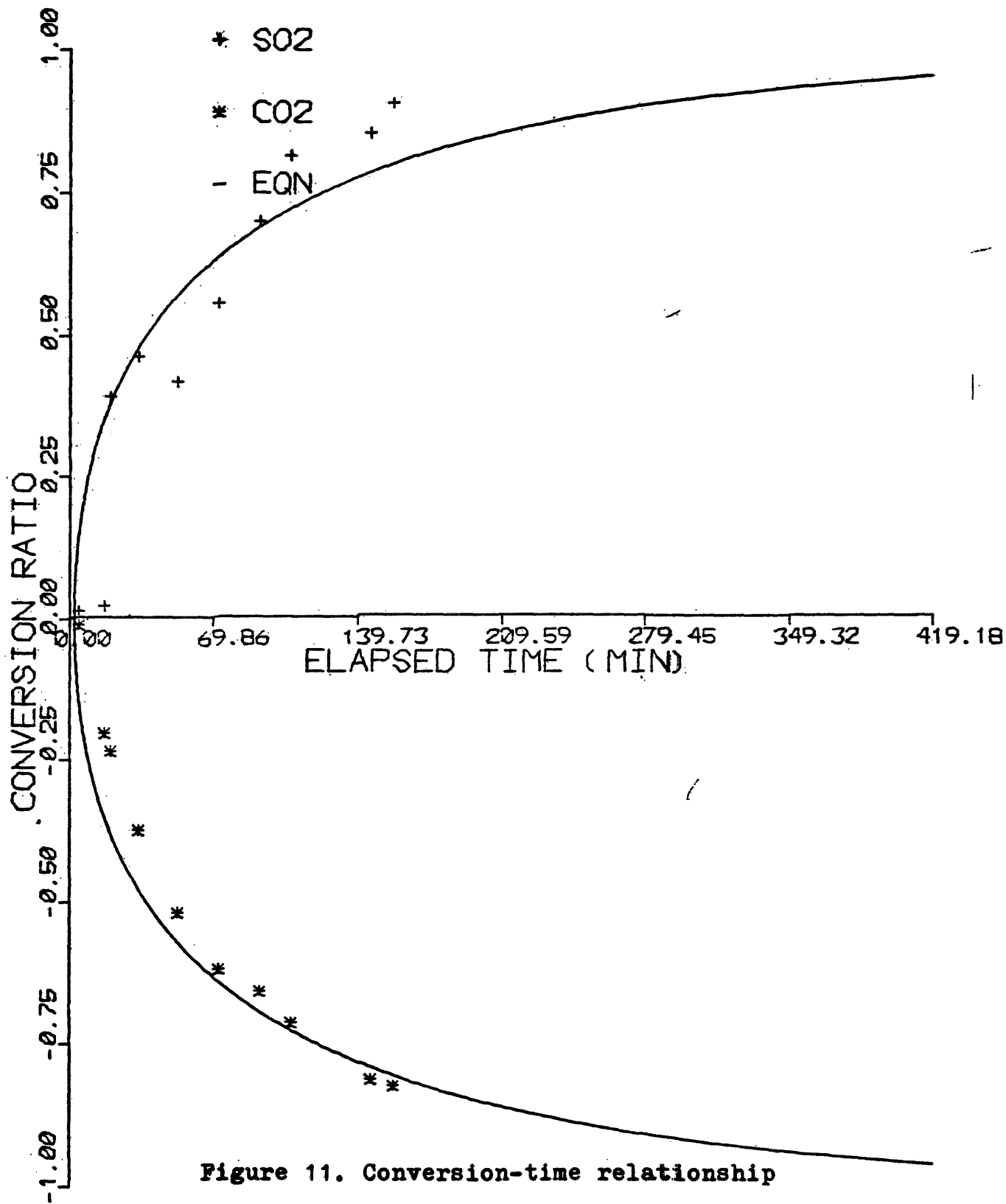


Figure 11. Conversion-time relationship of SO<sub>2</sub> and CO<sub>2</sub> for R 8.

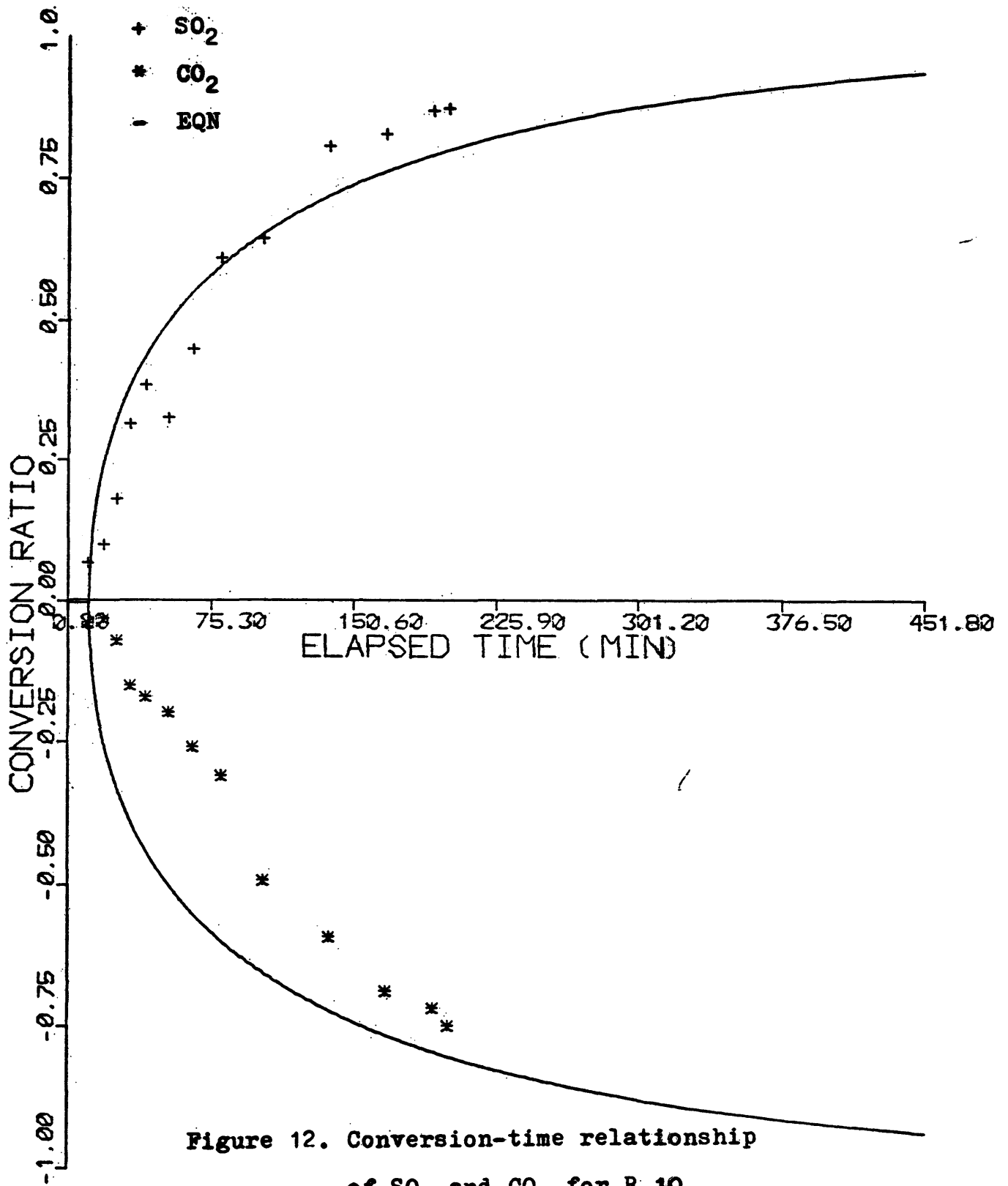


Figure 12. Conversion-time relationship of SO<sub>2</sub> and CO<sub>2</sub> for R 10.

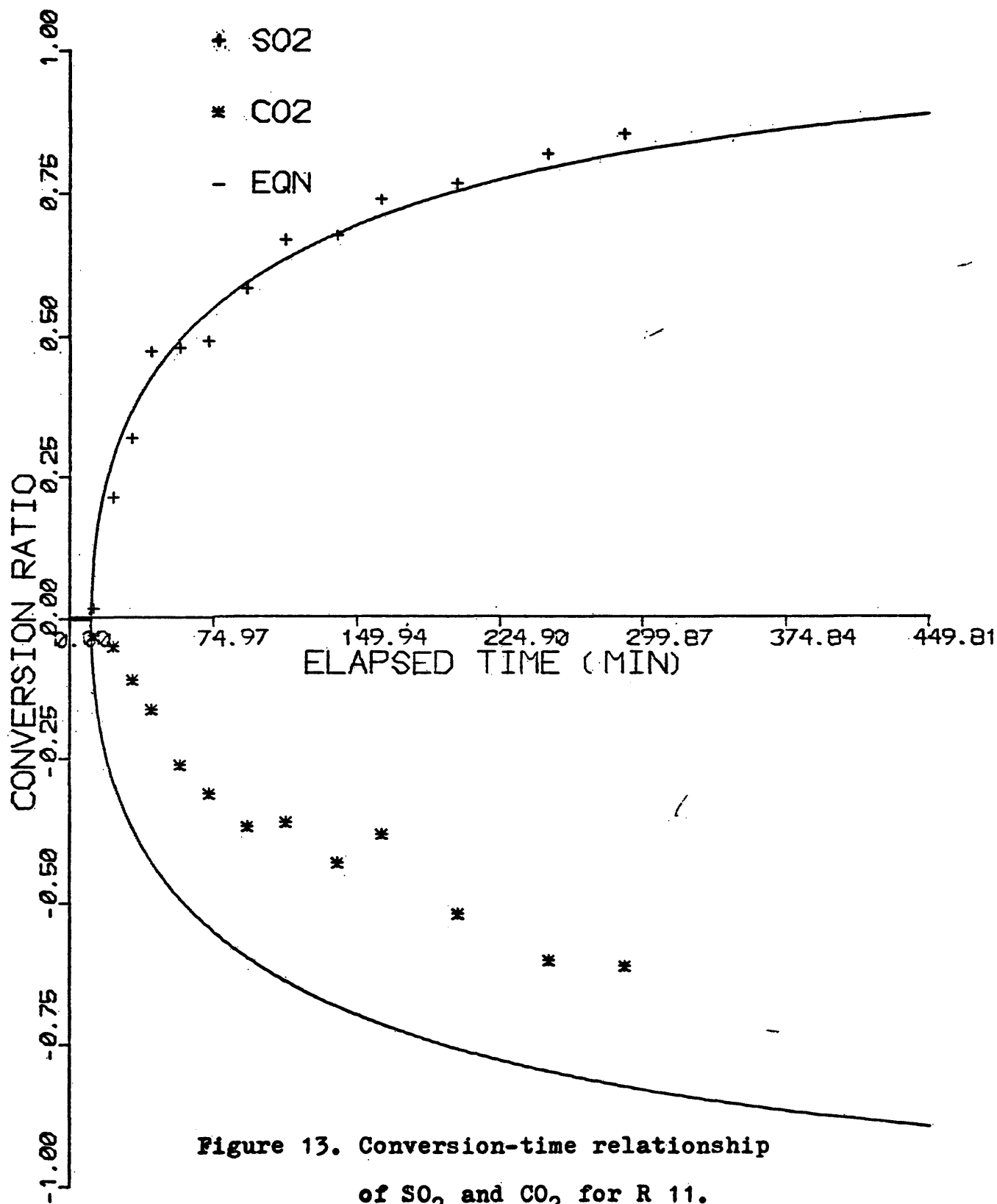


Figure 13. Conversion-time relationship of SO<sub>2</sub> and CO<sub>2</sub> for R 11.

### CONCLUSIONS

The following conclusions can be made from this study.

1. Moisture plays an important role in the  $\text{SO}_2$ -porous  $\text{Na}_2\text{CO}_3$  noncatalytic reaction system. When  $\text{H}_2\text{O}$  is present, the chemical reaction is very rapid and pore diffusion limits the overall reaction rate. Otherwise, the chemical reaction step controls the reaction system in the absence of  $\text{H}_2\text{O}$ .

2. The effective diffusivity of  $\text{SO}_2$  in  $\text{SO}_2$ - $\text{Na}_2\text{CO}_3$  multicomponent reaction system can be approximated by that of  $\text{SO}_2$  in air binary mixture.

3. Carbon dioxide and excess oxygen have no pronounced effect in this reaction system.

4. Tortuosity factor has a higher value at the higher pellet density or larger pore size.

5. From the mass balance relationship, the experimental data of  $\text{CO}_2$  showed that reaction (1) is the major reaction in a potential process of  $\text{SO}_2$  removal from stack gas by  $\text{Na}_2\text{CO}_3$  derived from nacholite.

### RECOMMENDATION FOR FURTHER STUDY

Based on the results in this study, the following further studies are recommended for the potential removal of  $\text{SO}_2$  by  $\text{Na}_2\text{CO}_3$ .

1. Difficulties arise when the sharp interface model is applied to reaction in a porous solid for the condition of chemical reaction control. If the sharp interface model is used to study either the activation energy or the stoichiometry of a gas-solid reaction there is a danger that experimental results will be misinterpreted. A grain model associated with the zone-reaction moving boundary can be to consider pore diffusion and the chemical reaction simultaneously. The grain model incorporates structural parameters such as grain size, porosity ( pore size distribution ), effective pore diffusion coefficient and allows the quantitative assessment of the role played by these in determining the overall reaction rate.

2. Consider unsteady-state heat transfer, geometrical instability, thermal instability, and the instability resulting from abrupt shiftings of the rate controlling step. Use of electron micrograph scans the structure within the solid particle before and after reactions.

3. Most of the work in gas-solid reaction has so far been carried out for only single particles. Under

similar reaction conditions, a model which can depict the rate expression for reaction in single particle may not be applicable in a packed bed (Sampath et al., 1973). A study in a packed bed is necessary for practice.

4. In order to broaden the applicability of this reaction system in industry,  $\text{NO}_x$  can be added to  $\text{SO}_2$  for the study of removal by a solid scrubbing agents.  $\text{NO}_x$  working as a catalyst in favor of removal  $\text{SO}_2$  has been reported (Werger et al., 1974). A simultaneous noncatalytic solid-gas reaction would be considered in such a situation (Wen and Wei, 1970). The unstable nature of  $\text{NO}_x$  in the atmosphere causes the problem in its analysis by gas chromatograph due to the rapid reactions  $\text{NO} + \frac{1}{2} \text{O}_2 \rightleftharpoons \text{NO}_2$  and  $\text{NO}_2 \rightleftharpoons \text{N}_2\text{O}_4$ .

LITERATURE CITED

- Ausman, J. M., and Watson, C. C., 1962, Mass transfer in a catalyst pellet during regeneration: Chem. Eng. Sci., v. 17, p. 323.
- Barron, C. H., and O'Hern, H. A., 1966, Reaction kinetics of sodium sulfite oxidation by the rapid-mixing method: Chem. Eng. Sci., v. 21, p. 397.
- Bird, B. R., Stewart, W. E., and Lightfoot, E. N., 1960, Transport phenomena: John Wiley & Sons, New York, p. 510.
- Eric, W., and Pedro, M., 1974, Sulfur dioxide adsorption on alkalized alumina adsorbents: Washington University St. Louis, Mo.
- Gokan, A. N., 1972, Measurement of diffusion in the ash layer in gas-solid reactions: Chem. Eng. Sci., v. 27, p. 1515.
- Hougen, A. O., Watson, K. M., and Ragatz, A. R., 1962, Chemical process principles part II, John Wiley & Sons, New York, p. 1003.
- Ishida, M., and Wen, C. Y., 1968, Comparison of kinetic and diffusional model for solid-gas reactions: AIChE J., v. 14, no. 2, p. 311.
- Krishnan, N. G., and Bartlett, R. W., 1973, Kinetics of sulfation of alkalized alumina: Atmospheric Environment, v. 7, no. 5, p. 575.
- Kwon, K. C., 1974, Ph. D. Thesis, Colorado School of Mines.
- \_\_\_\_\_, and Yesavage, V. F., 1976, Experimental and theoretical studies of the sodium carbonate-sulfur dioxide heterogenous reaction system in a single particle batch reactor: Colorado School of Mines.
- Levenspiel, O., 1962, Chemical reaction engineering: John Wiley & Sons, New York, p. 338-378.
- Meyer, B., and Carlson, C., 1971, Mechanism of sulfur dioxide adsorption on metal oxides, carbonates, and

hydroxides: Intl. Clean Air Cong., Second Proc., p. 835.

Sampath, B. S. and Hughes, R., 1973, Review of mathematical model in single particle gas-solid noncatalytic reactions: Chem. Eng. (London), no. 278, p. 485-492, 497.

Satterfield, C. N., 1970, Mass transfer in heterogeneous catalysis: MIT Press Cambridge, Mass..

Sherwood, K. T., Pigford, R. C., and Wilke, C. R., 1975, Mass transfer: McGraw Hill, New York.

Stern, C. A., 1968, Air pollution volume III : Academic Press, New York.

Weichman, B., 1974, The superior process for development of oil shale and associated minerals: Quarterly of the Colorado School of Mines, v. 69, no. 2, p. 25.

Wen, C. Y., Simultaneous noncatalytic solid-fluid reactions: AIChE J. v. 16, no. 5, p. 848.

**APPENDIX A**

**Generalized Regression Computer  
Program in Matrix Form**

This generalized regression computer program ( CALIBR-F10 ) is applicable in the multiple linear regression model

$$y = b_0 + b_1x_1 + \text{----} + b_kx_k, \quad (1A)$$

and the polynomial regression model

$$y = b_0 + b_1x + b_2x^2 + \text{----} + b_kx^k. \quad (2A)$$

Comparing both regression models, we can treat the terms,  $x^k$ 's, in equation (2A) as the corresponding terms,  $x_k$ 's, in equation (1A) when we run the computer program to solve the constant coefficients,  $b_k$ 's.

The Fortran IV computer program has been checked with the program written in Basic language. The results came out the same. Also a plotting program ( MATRIX-FOR ) can be added to plot the regression formulas into chart and to mark the experimental data.

### Mathematical Background

Suppose the experimenter has data of the type

$$\{(x_{1i}, x_{2i}, \text{----}, x_{ki}, y_i); i = 1, 2, \text{----} n \text{ and } n > k\}$$

where  $y_i$  is the observed response to the values  $x_{1i}$ ,  $x_{2i}$ , ----,  $x_{ki}$  of the  $k$  independent variables  $x_1$ ,  $x_2$ , ----,  $x_k$ .

Set the matrix  $\bar{X}$  as

$$\bar{X} = \left[ I, x_{1i}, x_{2i} \right] n \times (k + 1),$$

where  $I$  is unit vector,  $n$  is the data size, and  $k$  is the number of independent variables.

the matrix  $Y$  as

$$Y = \begin{bmatrix} y_1 \\ y_2 \\ \vdots \\ y_n \end{bmatrix} \quad n \times 1 ,$$

and the matrix  $B$  as

$$B = \begin{bmatrix} b_0 \\ b_1 \\ \vdots \\ b_k \end{bmatrix} \quad k \times 1$$

From the least square estimating, we have the normal equation in the matrix form.

$$AB = G \quad (3A)$$

where  $A = X^T X$  ,

and  $G = X^T Y$  .

If the matrix  $A$  is nonsingular, we can write the solution for the regression coefficient as

$$B = A^{-1}G \quad (4A)$$

### Example

In the calibration of gas chromatograph, we have the data of  $CO_2$  as following:

<u>VOL RATIO</u>	<u>PEAK RATIO</u>
0.189E-02	0.145E-02
0.378E-02	0.276E-02
0.567E-02	0.448E-02
0.757E-02	0.581E-02
0.946E-02	0.735E-02
0.114E-01	0.906E-02

Then

$$X = \begin{bmatrix} 1, \text{ peak ratio} \end{bmatrix} \quad 6 \times 2$$

$$Y = \begin{bmatrix} \text{vol. ratio} \end{bmatrix} \quad 6 \times 1$$

The result ends up:

$$B(1) = 0.209 \text{ E-03}$$

$$B(2) = 0.124 \text{ E+01}$$

i.e Vol. Ratio =  $2.09 \times 10^{-4}$  +  $1.24 \times$  Peak Ratio.

## • TY CALIBR.F10

[12:06:46]

```

      DIMENSION X(20,20),XTRAN(20,20),Y(20,20),A(20,20),G(20,20),
1     B(20,20)
      DATA IN,IOUT/9,10/
      READ(IN,5) IROW,JCOLM,NORUN
      DO 6 K=1,NORUN
      READ(IN,10) (Y(I,1),I=1,IROW)
      READ(IN,10) ((X(I,J),I=1,IROW),J=1,JCOLM)
C----- TRANPOSE X MATRIX-----
      DO 2 I=1,IROW
      DO 2 J=1,JCOLM
2     XTRAN(J,I)=X(I,J)
C----- START REGRESSION IN MATRIX FORM -----
      CALL MULTI(XTRAN,X,A,JCOLM,IROW,JCOLM)
      CALL MULTI(XTRAN,Y,G,JCOLM,IROW,1)
      CALL INVERS(A,JCOLM)
      CALL MULTI(A,G,B,JCOLM,JCOLM,1)
      WRITE(IOUT,15) IROW,JCOLM
      WRITE(IOUT,20)
      WRITE(IOUT,25) (Y(I,1),(X(I,J),J=2,JCOLM),I=1,IROW)
      DO 4 I=1,JCOLM
4     WRITE(IOUT,30) I,B(I,1)
6     CONTINUE
5     FORMAT(3I)
10    FORMAT(6F)
15    FORMAT(5X,' SAMPLE NO = ',I2,5X,' COLJMN NO = ',I2//)
20    FORMAT(5X,' VOL RATIO',5X,' PEAK RATIO'//)
25    FORMAT(5X,E10.3,5X,E10.3)
30    FORMAT(//5X,2HB(',I2,3H)= ',E10.3//)
      STOP
      END

```

```

      SUBROUTINE MULTI(A,U,T,M,N,L)
C----- T(M,L)=A(M,N)*U(N,L) -----
      DIMENSION A(20,20),U(20,20),T(20,20)
      DO 1 I=1,M
      DO 1 J=1,L
1     T(I,J)=0.
      DO 2 I=1,M
      DO 2 J=1,L
      DO 2 K=1,N
2     T(I,J)=A(I,K)*U(K,J)+T(I,J)
      RETURN
      END

```

```

      SUBROUTINE INVERS(DS,N)
C ---- INVERSE DS MATRIX N BY N ----
      DOUBLE PRECISION S(20,20)
      DIMENSION DS(20,20)
      DO 5 J=1,N
      DO 5 I=1,N
5     S(I,J)=DBLE(DS(I,J))
      S(1,N+1)=1.

```

```
DO 10 I=2,N
10 S(I,N+1)=0.
   NM1=N-1
   DO 40 K=1,N
   DO 20 J=1,N
20 S(N+1,J)=S(1,J+1)/S(1,1)
   DO 30 I=1,NM1
   DO 30 J=1,N
30 S(I,J)=S(I+1,J+1)-S(I+1,1)*S(N+1,J)
   DO 40 J=1,N
40 S(N,J)=S(N+1,J)
   DO 15 J=1,N
   DO 15 I=1,N
15 DS(I,J)=SNGL(S(I,J))
   RETURN
   END
```

• TY MATRIX.FOR  
[12:08:22]

```

      INTEGER OUT
      COMMON XSTART,YSTART,TITLEX(4),TITLEY(4),AXLEN,AYLEN,
C XZERO,YZERO,XXSYB(3),XXSYB(3),TITSYB(3),XD1(10),XD2(10),ZD(10)
      DIMENSION XX(20),YY(20),ZZ(20)
      DATA XSTART,YSTART/1.5,1.5/
      DATA XZERO,YZERO/0.,0./
      DATA AXLEN,AYLEN/7.,8./
      DATA XXSYB,XXSYB/2.,2.,2.,7.,7.5,8./
      DATA N,ND/13,6/
      IN=5
      OUT=6
400  FORMAT(3F7.5)
      READ(IN,400) (ZD(I),XD1(I),XD2(I),I=1,ND)
      WRITE(OUT,400) (ZD(I),XD1(I),XD2(I), I=1,ND)
      DO 1 I=1,N
      XX(I)=FLOAT(I)-1.
      YY(I)=2.81+0.77*XX(I)
      ZZ(I)=0.209+1.244*XX(I)
1    CONTINUE
      READ(IN,100) (TITLEX(J), J=1,4)
      READ(IN,100) (TITLEY(I), I=1,4)
100  FORMAT(4A5)
      DO 4 K=1,3
      READ(IN,40) TITSYB(K)
40   FORMAT(A5)
4    CONTINUE
      WRITE(OUT,100) (TITLEX(I),I=1,4)
      WRITE(OUT,100) (TITLEY(I), I=1,4)
      WRITE(OUT,300) (TITSYB(K),K=1,3)
300  FORMAT(A5)
      DO 2 J=1,N
      WRITE(OUT,200) (XX(J),YY(J),ZZ(J))
200  FORMAT(1X,3F10.3)
2    CONTINUE
      CALL PLOTTER(XX,YY,ZZ,N,ND)
      STOP
      END

```

```

SUBROUTINE PLOTTER(X,Y,Z,N,ND)
COMMON XSTART,YSTART,TITLEX(4),TITLEY(4),AXLEN,AYLEN,
C XZERO,YZERO,XXSYB(3),YSYB(3),TITSYB(3),XD1(10),XD2(10),ZD(10)
DIMENSION X(20),Y(20),Z(20)
XMAX=0.
YMAX=0.
DO 1 I=1,N
IF(ABS(X(I)).GT.XMAX) XMAX=ABS(X(I))
IF(ABS(Y(I)).GT.YMAX) YMAX=ABS(Y(I))
IF(ABS(Z(I)).GT.YMAX) YMAX=ABS(Z(I))
1 CONTINUE
DX=(XMAX-XZERO)/AXLEN
DY=(YMAX-YZERO)/AYLEN
DO 2 J=1,N
X(J)=X(J)/XMAX*AXLEN
Y(J)=Y(J)/YMAX*AYLEN
2 Z(J)=Z(J)/YMAX*AYLEN
KA=IPLOT(5)
IF(KA.NE.0) STOP
CALL PLOT(XSTART,YSTART,-3)
KCHANG=NEWPEN(2)
DO 3 K=1,N
3 CALL PLOT(X(K),Y(K),2)
CONTINUE
CALL PLOT(0.,0.,-3)
DO 4 L=1,N
4 CALL PLOT(X(L),Z(L),2)
CONTINUE
CALL PLOT(0.,0.,-3)
DO 5 M=1,ND
5 XD1(M)=XD1(M)/XMAX*AXLEN*1000
XD2(M)=XD2(M)/XMAX*AXLEN*1000
ZD(M)=ZD(M)/YMAX*AYLEN*1000
DO 6 I1=1,ND
6 CALL SYMBOL(XD1(I1),ZD(I1),0.14,1H+,0.,1)
CONTINUE
CALL PLOT(0.,0.,-3)
DO 7 J1=1,ND
7 CALL SYMBOL(XD2(J1),ZD(J1),0.14,1H*,0.,1)
CONTINUE
CALL PLOT(0.,0.,-3)
CALL AXIS(0.,0.,TITLEX,-20,AXLEN,0.,XZERO,DX)
CALL AXIS(0.,0.,TITLEY,20,AYLEN,90.,YZERO,DY)
DO 8 K1=1,3
8 CALL SYMBOL(XSYB(K1),YSYB(K1),0.14,TITSYB(K1),0.,5)
CONTINUE
CALL PLOT(0.,0.,999)
RETURN
END

```

•TY FOR08.DAT  
[12:04:38]

SAMPLE NO = 6      COLJMN NO = 2

VOL RATIO	PEAK RATIO
0.177E-02	0.170E-02
0.354E-02	0.314E-02
0.531E-02	0.504E-02
0.707E-02	0.701E-02
0.884E-02	0.819E-02
0.106E-01	0.112E-01

B( 1)= 0.458E-03

B( 2)= 0.949E+00

SAMPLE NO = 6      COLJMN NO = 2

VOL RATIO	PEAK RATIO
0.211E-02	0.268E-02
0.423E-02	0.430E-02
0.636E-02	0.578E-02
0.848E-02	0.754E-02
0.106E-01	0.952E-02
0.127E-01	0.117E-01

B( 1)= -0.775E-03

B( 2)= 0.118E+01

•TY FOR10.DAT  
[12:05:32]

SAMPLE NO = 6      COLJMN NO = 2

VOL RATIO	PEAK RATIO
0.189E-02	0.145E-02
0.378E-02	0.276E-02
0.567E-02	0.448E-02
0.757E-02	0.581E-02
0.946E-02	0.735E-02
0.114E-01	0.906E-02

B( 1)= 0.209E-03

B( 2)= 0.124E+01

SAMPLE NO = 6      COLJMN NO = 2

VOL RATIO	PEAK RATIO
0.189E-02	0.750E-03
0.378E-02	0.153E-02
0.567E-02	0.393E-02
0.757E-02	0.546E-02
0.946E-02	0.860E-02
0.114E-01	0.113E-01

B( 1)= 0.214E-02

B( 2)= 0.851E+00

## APPENDIX B

The Computer Program for Diffusivity and  
Plotting the Charts of Conversion-Time  
Relationship

The least square method to obtain the effective diffusivity, the time delay and the conversion-time relationship from equation (3) in the text was given in Kwon (1974) whose data was checked by this program. A two pens plotting subroutine ( SUBROUTINE PLOTTER ) was used to plot the conversion-time relationship for  $\text{CO}_2$  and  $\text{SO}_2$  with origin located at the center of left margin.

The input and output data files were presented in Appendix C. The plotting charts were shown in Figures 5-13 in text. Also in Table 4 was listed the variables in this program.

Table 4.

## List of Variables for the Computer Program

B1, B2	Constant coefficient in calibration curve of CO <sub>2</sub>
C1, C2	Constant coefficient in calibration curve of SO <sub>2</sub>
BS	Stoichiometric coefficient in reaction
CA	Bulk concentration of SO <sub>2</sub>
CAI	Initial bulk concentration of SO <sub>2</sub>
DE	Effective diffusivity of SO <sub>2</sub> (D <sub>e</sub> )
DEN	Density of Na <sub>2</sub> CO <sub>3</sub> particle (ρ)
DETD	D <sub>e</sub> * T <sub>d</sub>
MOLDEN	Molar density of Na <sub>2</sub> CO <sub>3</sub>
MWC	Molecular weight of Na <sub>2</sub> CO <sub>3</sub>
N	The number of theoretical data
ND	The sample size
PDE	$\bar{yT}/(T)^2$
PR1	Peak ratios of SO <sub>2</sub>
PR2	Peak ratios of CO <sub>2</sub>
PRESS	Operating pressure
R	Radius of core
RI	Radius of particle
RG	The constant in ideal gas law
RUN	The number of experiment
SXX	$\sum (x - \bar{X})^2$
SYI	$\sum (y - \bar{Y})^2$
SXY	$\sum (x - \bar{X}) (y - \bar{Y})$

SSE	$SYY - b * SXY$ where $b = SXY/SXX$
$S^2$	$SSE/(n-2)$
T	Time
TD	Time delay
TEMP	Operating temperature
TVALUE	T value in student t-distribution
VOL	Reactor volume
VR1	Volume ratio of $SO_2$
VR2	Volume ratio of $CO_2$
VRI	Initial volume ratio of $SO_2$
WTPART	Initial weight of particle
WTRP	Weight of the reacted particle
XA	Conversion ratio of $SO_2$
XB	Conversion ratio of particle
XC	Conversion ratio of $CO_2$
X(I)	$1/T(I)$
Y(I)	The y value in equation (9) in text.
YA(I)	$Y(I)/T(I)$

• TY THESIS.FOR  
[12:10:18]

```

REAL MWC,MWS,MOLDEN
INTEGER OUT
DIMENSION THETA(500),CAF(500),XAF(500),XBF(500),XCF(500),
C YEQF(500),TF(500)
DIMENSION X(20),PR1(20),PR2(20),VR1(20),VR2(20),CA(20),
C CC(20),THETA(20),XB(20),YEQ(20),Y(20),YA(20)
COMMON XSTART,YSTART,TITLX(4),TITLY(4),AXLEN,AYLEN,
C XZERO,YZERO,XXSYB(3),YSYB(3),TITSYB(3),T(20),XA(20),XC(20)
DATA TEMP,PRESS/393.0,24.757/
DATA MWC,MWS/106.0,142.05/
DATA VOL,BS/7010.0,1.0/
DATA RG/82.06/
DATA B1,B2/0.000459,0.949/
DATA C1,C2/-0.000775,1.18/
DATA XSTART,YSTART/1.5,5.5/
DATA XZERO,YZERO/0.,-4./
DATA AXLEN,AYLEN/7.,8./
DATA XSYB,YSYB/1.,1.,1.,3.,3.5,4./
IN=5
OUT=6
READ(IN,100) RUN
READ(IN,10)ND,N,TVALUE,VRCI
READ(IN,300) WTPART,DEN,URI
READ(IN,110) (TITLX(J), J=1,4)
READ(IN,110) (TITLY(I), I=1,4)
READ(IN,120) (TITSYB(K),K=1,3)
READ(IN,300) (T(I),PR1(I),PR2(I),I=1,ND)
PI=3.1416
OT=1./3.
RI=((3.*WTPART)/(4.*PI*DEN))*OT
MOLDEN=DEN/MWC
CAI=PRESS*URI/(29.92*RG*TEMP)
CCI=PRESS*VRCI/(29.92*RG*TEMP)
ABC=4.*PI*MOLDEN*RI**3.
YB=((3.*VOL*CAI*BS)/ABC-1.)*OT
WRITE(OUT,200) RUN
WRITE(OUT,20) RI,WTPART,DEN,URI,VRCI
WRITE(OUT,400) CAI,YB
WRITE(OUT,25)
WRITE(OUT,300) (T(I),PR1(I),PR2(I),I=1,ND)
C -----FIND DE BY LINEAR REGRESSION
SUMX=0.
SUMYA=0.
SUMXYA=0.
SUMX2=0.
SUMYA2=0.
SUMYT=0.
SUMY2=0.
SUMT2=0.
DO 1 K=1,ND
VR1(K)=B1+B2*PR1(K)
VR2(K)=C1+C2*PR2(K)

```

ARTHUR LAKES LIBRARY  
COLORADO SCHOOL of MINES  
GOLDEN, COLORADO 80401

```

CA(K)=PRESS*VR1(K)/(29.92*RG*TEMP)
CC(K)=PRESS*VR2(K)/(29.92*RG*TEMP)
THETA(K)=(1.-(CAI-CA(K))*3.*VOL*BS/ABC)**OT
XA(K)=1.-CA(K)/CAI
XB(K)=1.-THETA(K)**3.
XC(K)=0.-(CC(K)-CCI)/CAI
GO=THETA(K)
YEQ(K)=EQN(YB,GO)
Y(K)=RI**2.*MOLDEN/CAI/BS*YEQ(K)
YA(K)=Y(K)/T(K)
X(K)=1./T(K)
SUMX=SUMX+X(K)
SUMYA=SUMYA+YA(K)
SUMXYA=SUMXYA+X(K)*YA(K)
SUMX2=SUMX2+X(K)**2.
SUMYA2=SUMYA2+YA(K)**2.
SUMYT=SUMYT+Y(K)*T(K)
SUMY2=SUMY2+Y(K)**2.
SUMT2=SUMT2+T(K)**2.
1 CONTINUE
C ----- IF TD IS CONSTANT
SXX=SUMX2-SUMX**2./FLOAT(ND)
SYAYA=SUMYA2-SUMYA**2./FLOAT(ND)
SXYA=SUMXYA-SUMX*SUMYA/FLOAT(ND)
DETD=SXYA/SXX
DE=SUMYA/FLOAT(ND)-DETD*SUMX/FLOAT(ND)
TD=-DETD/DE
SSE=SYAYA-DETD*SXYA
S=SQRT(SSE/FLOAT(ND-2))
RDE=TVALUE*S*SQRT(SUMX2)/SQRT(FLOAT(ND)*SXX)
UDE=DE+RDE
LDE=DE-RDE
C ----- IF TD NOT CONSTANT
PDE=SUMYT/SUMT2
PS=SQRT(SUMY2/FLOAT(ND-1)-SUMTY**2./FLOAT(ND-1)/SUMT2)
PUDE=PDE+TVALUE*PS/SQRT(SUMT2)
PLDE=PDE-TVALUE*PS/SQRT(SUMT2)
WRITE(OUT,750)
WRITE(OUT,800) DE,S,UDE,LDE,TD
WRITE(OUT,700) PDE,PS,PUDE,PLDE
WRITE(OUT,850)
WRITE(OUT,900) (T(I),CA(I),XA(I),XB(I),XC(I),I=1,ND)
C ----- THEORETICAL RESULTS
XBF(1)=0.0
DO 2 I=1,N
J=I-1
THETAF(I)=(1.-XBF(I))*OT
CAF(I)=CAI-ABC*(1.-THETAF(I)**3.)/(3.*VOL*BS)
IF(CAF(I).LT.0.0) GO TO 940
XAF(I)=1.-CAF(I)/CAI
XCF(I)=0.-XAF(I)
GOF=THETAF(I)
YEQF(I)=EQN(YB,GOF)

```

```

TF(I)=RI**2.*MOLDEN/CAI/BS/DE*YEQF(I)
TIME=350.0
IF(TF(I).GE.TIME) GO TO 940
 2 XBF(I+1)=XBF(I)+1.0/FLOAT(N)
940 WRITE(OUT,950)
    WRITE(OUT,900) (TF(I),CAF(I),XAF(I),XBF(I),XCF(I),I=1,161,8)
    CALL PLOTTER(TF,XAF,XCF,J,ND)
10  FORMAT(1X,2I5,2F10.5)
20  FORMAT(' RI=',F6.3,1X,'WTPART= ',F4.3,1X,'DEN= ',F6.3/
C ' VRI=',F7.6,1X,'VRCI= ',F7.6//)
25  FORMAT(// ' EXP TIME    PR(1)    PR(2) ')
100  FORMAT(1X,A5)
110  FORMAT(4A5)
120  FORMAT(1X,A5)
200  FORMAT(' THE NUMBER OF TEST IS ',A5//)
300  FORMAT(F10.3,2F10.6)
400  FORMAT(' CAI= ',E11.4,5X,' YB= ',F10.6)
700  FORMAT(10X,4F11.6/)
750  FORMAT(/10X,' INTRA DIFF   STD ERROR   UPR DIFF   LWR DIFF
C TIME DELAY ')
800  FORMAT(1X,9HTD=CONST ,5F11.6)
850  FORMAT(5X,' RXN TIME   CONC SO2   RXN % SO2   RXN % PART   YIELD
C % CO2 '/')
900  FORMAT(5X,F11.6,E11.4,3F11.6)
950  FORMAT(15X,' THEORETICAL RESULTS '/')
    CALL PLOT(0.,0.,999)
    STOP
    END

```

```

FUNCTION EQN(YB,THETA)
AA=YB**3.+1.
BB=SQRT(3.)*YB
A=ALOG(AA*(YB+THETA)**3./((YB+1.)*3.*(YB**3.+THETA**3.)))
B=ATAN((2.-YB)/BB)-ATAN((2.*THETA-YB)/BB)
C=ALOG(AA/(YB**3.+THETA**3.))
1 EQN=AA/6./YB*A+AA*B/BB-AA*C/3.
RETURN
END

```

```

SUBROUTINE PLOTTER(X,Y,Z,N,ND)
DIMENSION X(500),Y(500),Z(500)
COMMON XSTART,YSTART,TITLEX(4),TITLEY(4),AXLEN,AYLEN,
C XZERO,YZERO,XSYB(3),YSYB(3),TITSYB(3),T(20),XA(20),XC(20)
XMAX=0.
YMAX=0.
DO 9 K1=1,ND
IF(ABS(T(K1)).GT.XMAX) XMAX=ABS(T(K1))
IF(ABS(XA(K1)).GT.YMAX) YMAX=ABS(XA(K1))
IF(ABS(XC(K1)).GT.YMAX) YMAX=ABS(XC(K1))
9 CONTINUE
DO 1 I=1,N
IF(ABS(X(I)).GT.XMAX) XMAX=ABS(X(I))
IF(ABS(Y(I)).GT.YMAX) YMAX=ABS(Y(I))
IF(ABS(Z(I)).GT.YMAX) YMAX=ABS(Z(I))
1 CONTINUE
DX=(XMAX-XZERO)/AXLEN
DY=(YMAX-XZERO)/ABS(YZERO)
DO 2 J=1,N
X(J)=X(J)/XMAX*AXLEN
Y(J)=Y(J)/YMAX*ABS(YZERO)
2 Z(J)=Z(J)/YMAX*ABS(YZERO)
KA=IPLOT(5)
IF(KA.NE.0) STOP
CALL PLOT(XSTART,YSTART,-3)
KCHANG=NEWPEN(2)
DO 3 K=1,N
CALL PLOT(X(K),Y(K),2)
3 CONTINUE
CALL PLOT(0.,0.,-3)
DO 4 L=1,N
CALL PLOT(X(L),Z(L),2)
4 CONTINUE
CALL PLOT(0.,0.,-3)
DO 5 M=1,ND
T(M)=T(M)/XMAX*AXLEN
XA(M)=XA(M)/YMAX*ABS(YZERO)
5 XC(M)=XC(M)/YMAX*ABS(YZERO)
DO 6 I1=1,ND
CALL SYMBOL(T(I1),XA(I1),0.14,1H+,0.,1)
6 CONTINUE
CALL PLOT(0.,0.,-3)
DO 7 J1=1,ND
CALL SYMBOL(T(J1),XC(J1),0.14,1H*,0.,1)
7 CONTINUE
CALL PLOT(0.,0.,-3)
CALL AXIS(0.,0.,TITLEX,-20,AXLEN,0.,XZERO,DX)
CALL AXIS(0.,YZERO,TITLEY,20,AYLEN,90.,-YMAX,DY)
DO 8 K1=1,3
CALL SYMBOL(XSYB(K1),YSYB(K1),0.14,TITSYB(K1),0.,5)
8 CONTINUE
RETURN
END

```

APPENDIX C

Raw Data and Calculated Results

Table 5. Raw Data and Calculated Results for R 2.

THE NUMBER OF TEST IS RUN 2

RI=.0546 WTPART=.874 DEN= 1.281  
 VRI=.006523 VRCI= 0.000000

CAI= 0.1673E-06 YB= -0.950148

EXP TIME	PR(1)	PR(2)
1.250	0.004830	0.000000
9.270	0.004460	0.000600
17.230	0.003460	0.000758
31.830	0.003340	0.001100
49.330	0.002400	0.001430
58.670	0.002030	0.001380
67.000	0.001670	0.001560
76.250	0.001610	0.001540

	INTRA DIFF	STD ERROR	UPR DIFF	LWR DIFF	TIME DELAY
TD=CONST	0.048773	0.020981	0.069258	0.000000	1.374263
	0.060089	3.061671	0.116599	0.003578	

RXN TIME	CONC SO2	RXN % SO2	RXN % PART	YIELD	% CO2
1.250000	0.1673E-06	0.000138	0.000020	-0.032055	
9.270000	0.1600E-06	0.043834	0.006234	-0.146534	
17.230000	0.1402E-06	0.161933	0.023031	-0.176680	
31.830000	0.1378E-06	0.176104	0.025046	-0.241933	
49.330000	0.1193E-06	0.287117	0.040835	-0.304896	
58.670000	0.1119E-06	0.330813	0.047049	-0.295356	
67.000000	0.1048E-06	0.373328	0.053096	-0.329699	
76.250000	0.1036E-06	0.380414	0.054104	-0.325883	

THEORETICAL RESULT

1.378780	0.1668E-06	0.002928	0.000416	-0.002928	
1.726520	0.1629E-06	0.026351	0.003748	-0.026351	
2.651201	0.1590E-06	0.049774	0.007079	-0.049774	
4.184825	0.1550E-06	0.073197	0.010410	-0.073197	
6.360544	0.1511E-06	0.096620	0.013742	-0.096620	
9.217044	0.1472E-06	0.120044	0.017073	-0.120044	
12.793474	0.1433E-06	0.143467	0.020404	-0.143467	
17.130949	0.1394E-06	0.166890	0.023736	-0.166890	
22.277427	0.1354E-06	0.190313	0.027067	-0.190313	
28.282070	0.1315E-06	0.213736	0.030398	-0.213736	
35.204381	0.1276E-06	0.237159	0.033730	-0.237159	
43.096199	0.1237E-06	0.260582	0.037061	-0.260582	
52.033274	0.1198E-06	0.284005	0.040392	-0.284005	
62.082670	0.1159E-06	0.307429	0.043724	-0.307429	
73.330936	0.1119E-06	0.330852	0.047055	-0.330852	
85.861078	0.1080E-06	0.354275	0.050386	-0.354275	
99.775744	0.1041E-06	0.377698	0.053718	-0.377698	
115.184166	0.1002E-06	0.401121	0.057049	-0.401121	
132.213058	0.9627E-07	0.424544	0.060380	-0.424544	

Table 6. Raw Data and Calculated Results for R 3.

THE NUMBER OF TEST IS RUN 3

RI= 0.426 WTPART= .435 DEN= 1.343  
 VRI=.007010 VRCI= 0.000000

CAI= 0.1799E-06 YB= -0.884836

EXP TIME	PR(1)	PR(2)
1.500	0.005460	0.000000
8.000	0.005390	0.000329
18.000	0.005070	0.000414
27.000	0.004140	0.000513
36.000	0.004750	0.000581
52.000	0.004350	0.000669
65.000	0.004610	0.000705
101.000	0.004050	0.000829
115.000	0.004270	0.000762

	INTRA DIFF	STD ERROR	UPR DIFF	LWR DIFF	TIME DELAY
TD=CONST	0.019018	0.017904	0.035028	0.000000	1.628640
	0.015221	1.096627	0.029554	0.000888	

RXN TIME	CONC SO2	RXN % SO2	RXN % PART	YIELD	% CO2
1.500000	0.1797E-06	0.000827	0.000254	-0.029815	
8.000000	0.1783E-06	0.008516	0.002617	-0.088199	
18.000000	0.1720E-06	0.043666	0.013416	-0.103283	
27.000000	0.1536E-06	0.145820	0.044800	-0.120852	
36.000000	0.1657E-06	0.078816	0.024215	-0.132919	
52.000000	0.1578E-06	0.122753	0.037714	-0.148536	
65.000000	0.1629E-06	0.094194	0.028939	-0.154924	
101.000000	0.1519E-06	0.155706	0.047838	-0.176930	
115.000000	0.1562E-06	0.131541	0.040413	-0.165040	

	THEORETICAL	RESULT			
	1.632401	0.1796E-06	0.001177	0.000362	-0.001177
	2.027327	0.1780E-06	0.010594	0.003255	-0.010594
	3.064341	0.1763E-06	0.020011	0.006148	-0.020011
	4.755391	0.1746E-06	0.029429	0.009041	-0.029429
	7.121707	0.1729E-06	0.038846	0.011935	-0.038846
	10.175298	0.1712E-06	0.048263	0.014828	-0.048263
	13.925671	0.1695E-06	0.057680	0.017721	-0.057680
	18.405722	0.1678E-06	0.067097	0.020614	-0.067097
	23.618205	0.1661E-06	0.076514	0.023507	-0.076514
	29.589908	0.1644E-06	0.085931	0.026401	-0.085931

Continue

36,335194	0.1627E-06	0.095348	0.029294	-0.095348
43,871593	0.1610E-06	0.104765	0.032187	-0.104765
52,219141	0.1593E-06	0.114182	0.035080	-0.114182
61,406407	0.1576E-06	0.123600	0.037974	-0.123600
71,444347	0.1559E-06	0.133017	0.040867	-0.133017
82,361686	0.1542E-06	0.142434	0.043760	-0.142434
94,177519	0.1525E-06	0.151851	0.046653	-0.151851
106,915953	0.1509E-06	0.161268	0.049547	-0.161268
120,595771	0.1492E-06	0.170685	0.052440	-0.170685
135,251411	0.1475E-06	0.180102	0.055333	-0.180102
150,904943	0.1458E-06	0.189519	0.058226	-0.189519
167,578127	0.1441E-06	0.198936	0.061119	-0.198936
185,304930	0.1424E-06	0.208354	0.064013	-0.208354
204,111647	0.1407E-06	0.217771	0.066906	-0.217771
224,023481	0.1390E-06	0.227188	0.069799	-0.227188
245,084576	0.1373E-06	0.236605	0.072692	-0.236605
267,308544	0.1356E-06	0.246022	0.075586	-0.246022
290,746109	0.1339E-06	0.255439	0.078479	-0.255439
315,420280	0.1322E-06	0.264856	0.081372	-0.264856
341,372379	0.1305E-06	0.274273	0.084265	-0.274273
368,639977	0.1288E-06	0.283690	0.087158	-0.283690
397,260948	0.1271E-06	0.293107	0.090052	-0.293107

Table 7. Raw Data and Calculated Results for R 4.

THE NUMBER OF TEST IS RUN 4

RI= 0.440 WTPART= .457 DEN= 1.279  
 VRI=.007723 VRCI= 0.004774

CAI= 0.1983E-06 YB= -0.878333

EXP TIME	PR(1)	PR(2)
1.500	0.006400	0.003700
9.000	0.006020	0.003770
20.000	0.005150	0.004160
40.000	0.004430	0.004340
50.000	0.004400	0.004130
60.000	0.003650	0.004320
70.000	0.003700	0.005200
90.000	0.003730	0.004560
120.000	0.003690	0.004770

	INTRA DIFF	STD ERROR	UPR DIFF	LWR DIFF	TIME DELAY
TD=CONST	0.071181	0.026019	0.094201	0.009000	1.645441
	0.069067	4.769525	0.128889	0.009244	

RXN TIME	CONC SO2	RXN % SO2	RXN % PART	YIELD	% CO2
1.500000	0.1983E-06	-0.000000	0.000000	-0.004891	
9.000000	0.1978E-06	0.037862	0.012207	-0.016159	
20.000000	0.1736E-06	0.124547	0.040153	-0.078939	
40.000000	0.1594E-06	0.196286	0.063282	-0.107914	
50.000000	0.1588E-06	0.199275	0.064245	-0.074110	
60.000000	0.1440E-06	0.274004	0.088337	-0.104695	
70.000000	0.1449E-06	0.269022	0.086731	-0.246351	
90.000000	0.1455E-06	0.266033	0.085767	-0.143328	
120.000000	0.1447E-06	0.270018	0.087052	-0.177133	

Continue

THEORETICAL		RESULT		
1.647737	0.1979E-06	0.001701	0.000548	-0.001701
1.872588	0.1952E-06	0.015304	0.004934	-0.015304
2.463985	0.1925E-06	0.028907	0.009320	-0.028907
3.436168	0.1899E-06	0.042511	0.013705	-0.042511
4.800864	0.1872E-06	0.056114	0.018091	-0.056114
6.573163	0.1845E-06	0.069718	0.022477	-0.069718
8.766248	0.1818E-06	0.083321	0.026862	-0.083321
11.395199	0.1791E-06	0.096925	0.031248	-0.096925
14.476748	0.1764E-06	0.110528	0.035634	-0.110528
18.026553	0.1737E-06	0.124131	0.040019	-0.124131
22.063073	0.1710E-06	0.137735	0.044405	-0.137735
26.602467	0.1683E-06	0.151338	0.048791	-0.151338
31.665276	0.1656E-06	0.164942	0.053176	-0.164942
37.271247	0.1629E-06	0.178545	0.057562	-0.178545
43.441481	0.1602E-06	0.192149	0.061948	-0.192149
50.197884	0.1575E-06	0.205752	0.066333	-0.205752
57.563291	0.1548E-06	0.219356	0.070719	-0.219356
65.562234	0.1521E-06	0.232959	0.075105	-0.232959
74.222445	0.1494E-06	0.246563	0.079490	-0.246563
83.568302	0.1467E-06	0.260166	0.083876	-0.260166
93.629891	0.1440E-06	0.273770	0.088262	-0.273770
104.440537	0.1413E-06	0.287373	0.092647	-0.287373
116.029477	0.1386E-06	0.300976	0.097033	-0.300976
128.432970	0.1359E-06	0.314580	0.101419	-0.314580
141.686344	0.1332E-06	0.328183	0.105804	-0.328183
155.828789	0.1305E-06	0.341787	0.110190	-0.341787
170.901424	0.1278E-06	0.355390	0.114576	-0.355390
186.949839	0.1251E-06	0.368994	0.118961	-0.368994
204.018700	0.1224E-06	0.382597	0.123347	-0.382597
222.159691	0.1197E-06	0.396201	0.127733	-0.396201
241.426428	0.1170E-06	0.409804	0.132118	-0.409804
261.872913	0.1143E-06	0.423408	0.136504	-0.423408

Table 8. Raw Data and Calculated Results for R 5.

THE NUMBER OF TEST IS RUN 5

RECYCLED PAPER

RI= 0.433 WTPART= .435 DEN= 1.278  
 VRI=.006290 VRCI= 0.000000

CAI= 0.1614E-06 YB= -0.898072

EXP TIME	PR(1)	PR(2)
1.500	0.004430	0.000000
9.500	0.004350	0.000166
20.500	0.004340	0.000271
35.000	0.004320	0.000492
50.000	0.004230	0.000629
65.000	0.004210	0.000584
86.500	0.003920	0.000698
133.670	0.003410	0.000822
163.500	0.003310	0.000839
189.670	0.003510	0.000795
250.500	0.003460	0.000999
305.500	0.003530	0.001017
345.500	0.002470	0.001092
374.340	0.002180	0.001143
382.000	0.002640	0.001062

ARTHUR LAKES LIBRARY  
 COLORADO SCHOOL OF MINES  
 GOLDEN, COLORADO 80401

	INTRA DIFF	STD ERROR	UPR DIFF	LWR DIFF	TIME DELAY
TD=CONST	0.006237	0.004957	0.009193	0.000000	0.271566
	0.010220	2.461998	0.016776	0.003665	

RXN TIME	CONC SO2	RXN % SO2	RXN % PART	YIELD	% CO2
1.500000	0.1594E-06	0.012544	0.003458	-0.033227	
9.500000	0.1578E-06	0.022337	0.006158	-0.066058	
20.500000	0.1576E-06	0.023561	0.006495	-0.086824	
35.000000	0.1572E-06	0.026010	0.007170	-0.130532	
50.000000	0.1554E-06	0.037027	0.010207	-0.157627	
65.000000	0.1550E-06	0.039475	0.010882	-0.148728	
86.500000	0.1493E-06	0.074976	0.020669	-0.171274	
133.670000	0.1392E-06	0.137409	0.037880	-0.195798	
163.500000	0.1372E-06	0.149650	0.041255	-0.199160	
189.670000	0.1412E-06	0.125167	0.034505	-0.190458	
250.500000	0.1472E-06	0.131288	0.036193	-0.230804	
305.500000	0.1416E-06	0.122719	0.033830	-0.234364	
345.500000	0.1206E-06	0.252480	0.069603	-0.249197	
374.340000	0.1149E-06	0.287981	0.079389	-0.259283	
382.000000	0.1240E-06	0.231669	0.063865	-0.243264	

Continue

THEORETICAL		RESULT		
0.297912	0.1611E-06	0.001652	0.000455	-0.001652
2.393486	0.1590E-06	0.014870	0.004099	-0.014870
7.929839	0.1569E-06	0.028087	0.007743	-0.028087
17.003228	0.1547E-06	0.041304	0.011387	-0.041304
29.746327	0.1526E-06	0.054522	0.015030	-0.054522
46.270391	0.1505E-06	0.067739	0.018674	-0.067739
66.698384	0.1483E-06	0.080956	0.022318	-0.080956
91.175374	0.1462E-06	0.094174	0.025961	-0.094174
119.813597	0.1441E-06	0.107391	0.029605	-0.107391
152.786379	0.1419E-06	0.120608	0.033249	-0.120608
190.227669	0.1398E-06	0.133826	0.036892	-0.133826
232.323337	0.1377E-06	0.147043	0.040536	-0.147043
279.180821	0.1355E-06	0.160260	0.044180	-0.160260
331.028080	0.1334E-06	0.173478	0.047824	-0.173478
388.021450	0.1313E-06	0.186695	0.051467	-0.186695
450.364998	0.1291E-06	0.199912	0.055111	-0.199912

Table 9. Raw Data and Calculated Results for R 6.

## THE NUMBER OF TEST IS RUN 6

RI= 0.436 WTPART= .417 DEN= 1.204  
 VRI=.007451 VRCI= 0.000000

CAI= 0.1912E-06 YB= -0.870371

EXP TIME	PR(1)	PR(2)
1.500	0.006040	0.000000
11.020	0.005930	0.000000
20.660	0.005690	0.000000
41.500	0.005240	0.000000
60.000	0.004910	0.000000
80.000	0.005000	0.000000
110.000	0.004890	0.000000
140.000	0.004550	0.000000
180.000	0.004120	0.000000
248.000	0.004020	0.000000
294.000	0.003090	0.000000
364.000	0.002440	0.000000
432.000	0.002240	0.000000

	INTRA DIFF	STD ERROR	UPR DIFF	LWR DIFF	TIME DELAY
TD=CONST	0.018835	0.011727	0.026530	0.000000	1.755607
	0.031513	7.030915	0.052505	0.010521	

RXN TIME	CONC SO2	RXN % SO2	RXN % PART	YIELD	% CO2
1.500000	0.1912E-06	0.000027	0.000009	-0.028050	
11.020000	0.1890E-06	0.011394	0.003882	-0.028050	
20.660000	0.1843E-06	0.036196	0.012331	-0.028050	
41.500000	0.1754E-06	0.082700	0.028172	-0.028050	
60.000000	0.1688E-06	0.116803	0.039790	-0.028050	
80.000000	0.1706E-06	0.107502	0.036621	-0.028050	
110.000000	0.1684E-06	0.118870	0.040494	-0.028050	
140.000000	0.1617E-06	0.154006	0.052463	-0.028050	
180.000000	0.1532E-06	0.198443	0.067601	-0.028050	
248.000000	0.1513E-06	0.208777	0.071121	-0.028050	
294.000000	0.1329E-06	0.304885	0.103861	-0.028050	
364.000000	0.1200E-06	0.372057	0.126743	-0.028050	
432.000000	0.1161E-06	0.392726	0.133784	-0.028050	

Continue

THEORETICAL		RESULT		
1.774049	0.1908E-06	0.002158	0.000735	-0.002158
3.235816	0.1875E-06	0.019422	0.006616	-0.019422
7.113486	0.1842E-06	0.036686	0.012497	-0.036686
13.511445	0.1809E-06	0.053950	0.018378	-0.053950
22.540668	0.1776E-06	0.071214	0.024259	-0.071214
34.324769	0.1743E-06	0.088478	0.030141	-0.088478
48.991469	0.1710E-06	0.105742	0.036022	-0.105742
66.665599	0.1677E-06	0.123006	0.041903	-0.123006
87.503701	0.1644E-06	0.140270	0.047784	-0.140270
111.646777	0.1611E-06	0.157535	0.053665	-0.157535
139.262663	0.1578E-06	0.174799	0.059546	-0.174799
170.519608	0.1545E-06	0.192063	0.065427	-0.192063
205.621618	0.1512E-06	0.209327	0.071308	-0.209327
244.709564	0.1479E-06	0.226591	0.077189	-0.226591
288.044182	0.1446E-06	0.243855	0.083070	-0.243855
335.837704	0.1413E-06	0.261119	0.088951	-0.261119
388.325573	0.1380E-06	0.278383	0.094833	-0.278383
445.774597	0.1347E-06	0.295647	0.100714	-0.295647

Table 10. Raw Data and Calculated Results for R 7.

THE NUMBER OF TEST IS RUN 7

RI= 0.533 WTPART= .816 DEN= 1.283  
 VRI=.208130 VRCI= 0.000000

CAI= 0.2086E-06 YB= -0.932189

EXP TIME	PR(1)	PR(2)
1.830	0.006920	0.000000
12.000	0.006020	0.000000
35.500	0.005240	0.000000
58.000	0.004250	0.000000
91.500	0.004670	0.000000
130.000	0.003450	0.000000
160.000	0.003410	0.000000
231.500	0.001980	0.000000
293.000	0.001500	0.000000
358.000	0.001130	0.000000
391.000	0.001070	0.000000

	INTRA DIFF	STD ERROR	UPR DIFF	LWR DIFF	TIME DELAY
YD=CONST	0.038616	0.010698	0.046319	0.000000	1.931248
	0.045486	10.003695	0.077396	0.013577	

RXN TIME	CONC SO2	RXN % SO2	RXN % PART	YIELD	% CO2
1.830000	0.2086E-06	0.000197	0.000037	-0.025707	
12.000000	0.1938E-06	0.085437	0.016229	-0.025707	
35.500000	0.1754E-06	0.159311	0.030261	-0.025707	
58.000000	0.1558E-06	0.253075	0.048071	-0.025707	
91.500000	0.1641E-06	0.213296	0.040515	-0.025707	
130.000000	0.1400E-06	0.328844	0.062463	-0.025707	
160.000000	0.1392E-06	0.332632	0.063183	-0.025707	
231.500000	0.1110E-06	0.468069	0.088909	-0.025707	
293.000000	0.1015E-06	0.513530	0.097544	-0.025707	
358.000000	0.9417E-07	0.548573	0.104201	-0.025707	
391.000000	0.9298E-07	0.554256	0.105280	-0.025707	

Continue

THEORETICAL		RESULT		
1.942261	0.2079E-06	0.003270	0.000621	-0.003270
2.691785	0.2025E-06	0.029430	0.005593	-0.029430
4.697840	0.1970E-06	0.055589	0.010559	-0.055589
8.034612	0.1915E-06	0.081749	0.015528	-0.081749
12.794540	0.1861E-06	0.107908	0.020497	-0.107908
19.068473	0.1806E-06	0.134068	0.025466	-0.134068
26.958123	0.1752E-06	0.160227	0.030435	-0.160227
36.577752	0.1697E-06	0.186387	0.035404	-0.186387
48.051375	0.1643E-06	0.212546	0.040373	-0.212546
61.510929	0.1588E-06	0.238706	0.045342	-0.238706
77.110899	0.1533E-06	0.264865	0.050311	-0.264865
95.016278	0.1479E-06	0.291025	0.055280	-0.291025
115.414064	0.1424E-06	0.317184	0.060249	-0.317184
138.511368	0.1370E-06	0.343344	0.065218	-0.343344
164.545374	0.1315E-06	0.369503	0.070187	-0.369503
193.776959	0.1261E-06	0.395663	0.075156	-0.395663
226.503748	0.1206E-06	0.421822	0.080125	-0.421822
263.070663	0.1151E-06	0.447982	0.085094	-0.447982
303.861855	0.1097E-06	0.474141	0.090063	-0.474141
349.332966	0.1042E-06	0.500301	0.095032	-0.500301
400.004765	0.9878E-07	0.526461	0.100001	-0.526461
456.490620	0.9332E-07	0.552620	0.104970	-0.552620

Table 11. Raw Data and Calculated Results for R 8.

THE NUMBER OF TEST IS RUN 8

RI= 0.497 WTPART= .625 DEN= 1.218  
 VRI=.007000 VRCI= 0.000000

CAI= 0.1796E-06 YB= -0.923055

EXP TIME	PR(1)	PR(2)
2.000	0.005450	0.000000
14.330	0.005370	0.001070
17.330	0.002030	0.001240
31.000	0.001390	0.002020
50.000	0.001790	0.002840
70.000	0.000530	0.003390
90.000	-0.000770	0.003610
105.000	-0.001820	0.003920
143.500	-0.002180	0.004480
154.500	-0.002660	0.004540

	INTRA DIFF	STD ERROR	UPR DIFF	LWR DIFF	TIME DELAY
TD=CONST	0.458197	0.230009	0.639808	0.000000	2.229826
	0.613920	57.030087	1.085956	0.141883	

RXN TIME	CONC SO2	RXN % SO2	RXN % PART	YIELD % CO2
2.000000	0.1795E-06	0.000500	0.000107	-0.029857
14.330000	0.1779E-06	0.009300	0.001986	-0.220011
17.330000	0.1119E-06	0.376700	0.080436	-0.250223
31.000000	0.9930E-07	0.447100	0.095468	-0.388840
50.000000	0.1072E-06	0.403100	0.086073	-0.534566
70.000000	0.8231E-07	0.541700	0.115668	-0.632309
90.000000	0.5663E-07	0.684700	0.146202	-0.671406
105.000000	0.3588E-07	0.800200	0.170865	-0.726497
143.500000	0.2877E-07	0.839800	0.179321	-0.826017
154.500000	0.1929E-07	0.892600	0.190595	-0.836680

Continue

THEORETICAL		RESULT		
2.231723	0.1738E-06	0.004507	0.000962	-0.004507
2.377956	0.1723E-06	0.040564	0.008661	-0.040564
2.773776	0.1658E-06	0.076620	0.016366	-0.076620
3.441389	0.1594E-06	0.112676	0.024059	-0.112676
4.406428	0.1529E-06	0.148733	0.031759	-0.148733
5.697827	0.1464E-06	0.184789	0.039458	-0.184789
7.347760	0.1399E-06	0.220845	0.047157	-0.220845
9.393798	0.1335E-06	0.256902	0.054856	-0.256902
11.878983	0.1270E-06	0.292958	0.062555	-0.292958
14.853425	0.1205E-06	0.329014	0.070254	-0.329014
18.375494	0.1140E-06	0.365071	0.077953	-0.365071
22.513085	0.1076E-06	0.401127	0.085652	-0.401127
27.348433	0.1011E-06	0.437184	0.093351	-0.437184
32.978565	0.9461E-07	0.473240	0.101050	-0.473240
39.522628	0.8813E-07	0.509296	0.108749	-0.509296
47.126100	0.8166E-07	0.545353	0.116448	-0.545353
55.971795	0.7518E-07	0.581409	0.124147	-0.581409
66.291844	0.6870E-07	0.617466	0.131846	-0.617466
78.386493	0.6223E-07	0.653522	0.139545	-0.653522
92.657342	0.5575E-07	0.689578	0.147244	-0.689578
109.653622	0.4928E-07	0.725635	0.154943	-0.725635
130.159164	0.4280E-07	0.761691	0.162642	-0.761691
155.346172	0.3632E-07	0.797747	0.170341	-0.797747
187.080322	0.2985E-07	0.833804	0.178040	-0.833804
228.613661	0.2337E-07	0.869860	0.185739	-0.869860
286.413242	0.1690E-07	0.905917	0.193438	-0.905917
376.617321	0.1042E-07	0.941973	0.201137	-0.941973

Table 12. Raw Data and Calculated Results for R 10.

THE NUMBER OF TEST IS RN 10

RI= 0.422 WTPART= .337 DEN= 1.073  
 VRI=.005783 VRCI= -0.000280

CAI= 0.1484E-06 YB= -0.876269

EXP TIME	PR(1)	PR(2)
8.000	0.005260	0.000676
16.000	0.005060	0.000641
23.000	0.004570	0.000834
30.000	0.003760	0.001229
38.000	0.003340	0.001325
50.000	0.003690	0.001460
63.000	0.002950	0.001759
78.000	0.001970	0.002007
100.000	0.001760	0.002911
135.000	0.000770	0.003401
165.000	0.000640	0.003869
190.000	0.000390	0.004011
198.000	0.000360	0.004166

	INTRA DIFF	STD ERROR	UPR DIFF	LWR DIFF	TIME DELAY
TD=CONST	0.718492	0.262099	0.932471	0.000000	10.977077
	0.867289	98.162864	1.431769	0.302809	

RXN TIME	CONC SO2	RXN % SO2	RXN % PART	YIELD	% CO2
8.000000	0.1399E-06	0.057455	0.018797	-0.052340	
16.000000	0.1350E-06	0.090275	0.029534	-0.045198	
23.000000	0.1231E-06	0.170685	0.055841	-0.084579	
30.000000	0.1033E-06	0.303607	0.099328	-0.165177	
38.000000	0.9310E-07	0.372530	0.121877	-0.184766	
50.000000	0.1016E-06	0.315094	0.103286	-0.212312	
63.000000	0.8361E-07	0.436529	0.142815	-0.273322	
78.000000	0.5974E-07	0.597349	0.195423	-0.323925	
100.000000	0.5463E-07	0.631810	0.206753	-0.508383	
135.000000	0.3053E-07	0.794271	0.259853	-0.608366	
165.000000	0.2736E-07	0.815624	0.266333	-0.703860	
190.000000	0.2127E-07	0.856630	0.280255	-0.732834	
198.000000	0.2054E-07	0.861553	0.281865	-0.764461	

Continue

THEORETICAL RESULT

10.978724	0.1478E-06	0.004058	0.001327	-0.004058
11.115075	0.1430E-06	0.036518	0.011947	-0.036518
11.483102	0.1381E-06	0.068978	0.022567	-0.068978
12.102596	0.1333E-06	0.101438	0.033187	-0.101438
12.995794	0.1285E-06	0.133899	0.043806	-0.133899
14.187504	0.1237E-06	0.166359	0.054426	-0.166359
15.705651	0.1189E-06	0.198819	0.065246	-0.198819
17.581310	0.1141E-06	0.231279	0.075665	-0.231279
19.850387	0.1092E-06	0.263740	0.086285	-0.263740
22.553266	0.1044E-06	0.296200	0.096905	-0.296200
25.736463	0.9961E-07	0.328660	0.107524	-0.328660
29.453392	0.9479E-07	0.361121	0.118144	-0.361121

33.766503	0.8998E-07	0.393581	0.128764	-0.393581
38.747780	0.8516E-07	0.426041	0.139383	-0.426041
44.482833	0.8035E-07	0.458501	0.150203	-0.458501
51.073264	0.7553E-07	0.490962	0.160623	-0.490962
58.640464	0.7071E-07	0.523422	0.171242	-0.523422
67.332788	0.6590E-07	0.555882	0.181862	-0.555882
77.331932	0.6108E-07	0.588342	0.192482	-0.588342
88.865454	0.5626E-07	0.620803	0.203101	-0.620803
102.221452	0.5145E-07	0.653263	0.213721	-0.653263
117.774962	0.4663E-07	0.685723	0.224341	-0.685723
136.223813	0.4182E-07	0.718183	0.234961	-0.718183
157.649393	0.3700E-07	0.750644	0.245580	-0.750644
183.621347	0.3218E-07	0.783104	0.256200	-0.783104
215.383154	0.2737E-07	0.815564	0.266820	-0.815564
255.223587	0.2255E-07	0.848025	0.277439	-0.848025
307.099693	0.1773E-07	0.880485	0.288059	-0.880485
378.791843	0.1292E-07	0.912945	0.298679	-0.912945

"WASTE NOT BOND" IS A TRADEMARK OF SHADE INC.

Table 13. Raw Data and Calculated Results for R 11.

RECYCLED PAPER - "WASTE NOT BOND" - THIS FORM IS REC

THE NUMBER OF TEST IS RN 11

RI= 0.328 WTPART= .157 DEN= 1.065

VRI=.005972 VRCI= -0.000460

CAI= 0.1532E-06 YB= -0.650140

EXP TIME	PR(1)	PR(2)
10.000	0.005770	0.000501
20.000	0.004540	0.000602
30.000	0.003880	0.000904
40.000	0.002920	0.001170
55.000	0.002880	0.001660
70.000	0.002800	0.001911
90.000	0.002220	0.002200
110.000	0.001680	0.002163
137.000	0.001630	0.002522
160.000	0.001230	0.002268
200.000	0.001060	0.002984
248.000	0.000730	0.003400
288.000	0.000510	0.003450

TD=CONST	INTRA DIFF	STD ERROR	UPR DIFF	LWR DIFF	TIME DELAY
	2.006960	0.303099	2.249733	0.000000	11.226733
	2.015505	298.502033	3.304138	0.726873	

RXN TIME	CONC SO2	RXN % SO2	RXN % PART	YIELD	% CO2
10.000000	0.1523E-06	0.006241	0.004526	-0.046246	
20.000000	0.1223E-06	0.201698	0.146271	-0.066202	
30.000000	0.1063E-06	0.306577	0.222329	-0.125874	
40.000000	0.8238E-07	0.459129	0.332959	-0.178433	
55.000000	0.8190E-07	0.465486	0.337569	-0.275251	
70.000000	0.7995E-07	0.478198	0.346788	-0.324846	
90.000000	0.6583E-07	0.570365	0.413627	-0.381949	
110.000000	0.5268E-07	0.656175	0.475857	-0.374638	
137.000000	0.5147E-07	0.664121	0.481619	-0.445573	

Continue

RECYCLED PAPER - "WASTE NOT BOND" - THIS FORM IS RECYCLABLE "WASTE NOT BOND" IS A TRADEMARK OF SHADE INC.

160.000000	0.4173E-07	0.727684	0.527715	-0.395385
200.000000	0.3759E-07	0.754699	0.547306	-0.536859
248.000000	0.2955E-07	0.807138	0.585335	-0.619056
288.000000	0.2419E-07	0.842098	0.610688	-0.628935

	THEORETICAL	RESULT		
11.228091	0.1527E-06	0.003644	0.002643	-0.003644
11.340720	0.1482E-06	0.032798	0.023785	-0.032798
11.645682	0.1437E-06	0.061951	0.044927	-0.061951
12.161018	0.1393E-06	0.091105	0.066069	-0.091105
12.906689	0.1348E-06	0.120258	0.087211	-0.120258
13.905018	0.1303E-06	0.149411	0.108353	-0.149411
15.181220	0.1259E-06	0.178565	0.129495	-0.178565
16.763442	0.1214E-06	0.207718	0.150637	-0.207718
18.683714	0.1169E-06	0.236872	0.171779	-0.236872
20.978271	0.1125E-06	0.266025	0.192921	-0.266025
23.688365	0.1080E-06	0.295179	0.214063	-0.295179
26.861227	0.1035E-06	0.324332	0.235205	-0.324332
30.551174	0.9906E-07	0.353485	0.256347	-0.353485
34.820994	0.9460E-07	0.382639	0.277489	-0.382639
39.743694	0.9013E-07	0.411792	0.298631	-0.411792
45.404545	0.8566E-07	0.440946	0.319773	-0.440946
51.904067	0.8119E-07	0.470099	0.340915	-0.470099
59.361662	0.7673E-07	0.499253	0.362057	-0.499253
67.920072	0.7226E-07	0.528406	0.383199	-0.528406
77.751839	0.6779E-07	0.557560	0.404341	-0.557560
89.067863	0.6333E-07	0.586713	0.425483	-0.586713
102.128411	0.5886E-07	0.615866	0.446625	-0.615866
117.260004	0.5439E-07	0.645020	0.467767	-0.645020
134.878185	0.4993E-07	0.674173	0.488909	-0.674173
155.522169	0.4546E-07	0.703327	0.510051	-0.703327
179.906755	0.4099E-07	0.732480	0.531193	-0.732480
209.035489	0.3652E-07	0.761634	0.552335	-0.761634
244.187698	0.3206E-07	0.790787	0.573477	-0.790787
287.460487	0.2759E-07	0.819940	0.594619	-0.819940
341.925999	0.2312E-07	0.849094	0.615761	-0.849094
412.737743	0.1866E-07	0.878247	0.636903	-0.878247